

Universal horizons and black hole spectroscopy in gravitational theories with broken Lorentz symmetry

Chao Zhang^{a,b,c,d,*}, Anzhong Wang^{e,†} and Tao Zhu^{a,b‡}

^a Institute for theoretical physics and cosmology,

Zhejiang University of Technology, Hangzhou, 310032, China

^b United Center for Gravitational Wave Physics (UCGWP),

Zhejiang University of Technology, Hangzhou, 310032, China

^c College of Information Engineering, Zhejiang University of Technology, Hangzhou, 310032, China

^d Department of Physics, Faculty of Science, Tokyo University of Science,

1-3, Kagurazaka, Shinjuku-ku, Tokyo 162-8601, Japan

^e GCAP-CASPER, Physics Department, Baylor University, Waco, Texas, 76798-7316, USA

(Dated: September 13, 2022)

The violation of Lorentz invariance (LI) in gravitational theories, which allows superluminal propagations, dramatically alters the causal structure of the spacetime and modifies the notion of black holes. In particular, instead of metric horizons, now *universal horizons* define the boundaries of black holes, within which a particle cannot escape to spatial infinities even with an infinitely large speed. Then, a natural question is how the quasi-normal modes (QNMs) of a black hole are modified, if one considers the universal horizon as its causal boundary. In this paper, we study in detail this problem in Einstein-aether theory, a vector-tensor theory that violates LI but yet is self-consistent and satisfies all observations carried out so far. Technically, this poses several challenges, including singularities of the perturbation equations across metric horizons and proper identifications of ingoing modes at universal horizons. After overcoming these difficulties, we show that the QNMs of the Schwarzschild black hole, also a solution of Einstein-aether theory, consist of two parts, the metric and aether parts. The QNMs of the metric perturbations are quite similar to those obtained in general relativity and are consistent with current observations of gravitational waves. But the ones from aether perturbations are different, and our numerical studies indicate that they are even not stable. The latter is consistent with our previous studies, which showed that the stealth Schwarzschild black hole suffers a Laplacian instability along the angular direction. The method and techniques developed in this paper can be applied to the studies of QNMs in other theories of gravity with broken LI.

I. INTRODUCTION

The detection of the first gravitational wave (GW) from the coalescence of two massive black holes (BHs) by advanced LIGO marked the beginning of a new era — *the GW astronomy* [1]. Following this observation, about 90 GW events have been identified by the LIGO/Virgo/KAGRA (LVK) scientific collaborations (see, e.g., [2–5]). In the future, more ground- and space-based GW detectors will be constructed [6, 7], which will enable us to probe signals with a much wider frequency band and larger distances. This triggered the interests on the quasi-normal mode (QNM) of black holes, as GWs emitted in the ringdown phase can be considered as the linear combination of these individual modes [8, 9].

From the classical point of view, QNMs of black holes are eigenmodes of dissipative systems. The information contained in QNMs provide the keys in revealing whether BHs are ubiquitous in our universe, and more important whether general relativity (GR) is the correct theory to

describe gravity even in the strong field regime [10]. Basically, a QNM frequency ω contains two parts, the real and imaginary parts. Its real part gives the frequency of vibration while its imaginary part provides the damping time.

In GR, according to the no-hair theorem, an isolated and stationary BH is completely characterized by only three quantities, mass, angular momentum and electric charge. Astrophysically, we expect BHs to be neutral, so they are uniquely described by the Kerr solution. Then, the QNM frequencies and damping times will depend only on the mass and angular momentum of the finally formed BH. Clearly, to extract physics from the ringdown phase, at least two QNMs are needed. This will require the signal-to-noise ratio (SNR) to be of the order 100 [9]. Although such high SNRs are not achievable right now, it has been shown that they may be achievable once the advanced LIGO, Virgo and KAGRA reach their fully designed sensitivities. In any case, it is certain that they will be detected by the ground-based third-generation detectors, such as Cosmic Explorer [11] and the Einstein Telescope [12], as well as the space-based detectors, including LISA [13], TianQin [14], Taiji [15], and DECIGO [16].

QNMs in GR have been studied extensively [17], including scalar, vector and tensor perturbations [18]. Such calculations have been extended from the Schwarzschild

* chao123@zjut.edu.cn

† Anzhong_Wang@baylor.edu; Corresponding author

‡ zhut05@zjut.edu.cn

BH [19] to other more general cases, e.g., the Kerr BH [20, 21]. In this procedure, several different techniques of computations of QNMs were developed. For instance, the Wentzel-Kramers-Brillouin (WKB) approach [22–25], the finite difference method (FDM) [26], the continued fraction method [27], the shooting method [19], the matrix method [28], and so on [29–31]. Some of these methods have been also applied to modified theories of gravity [32, 33]. Additionally, some special approximations, e.g., the eikonal limit, have also been extensively explored, see, for example, [34] and references therein.

In this paper, we shall focus on the QNMs of black holes in Einstein-aether theory (α -theory) [35]. Such studies are well motivated. In particular, the theory is self-consistent, such as free of ghosts and instability [36], and satisfies all the experimental tests carried out so far [37]. Its Cauchy problem is also well posed [38], and energy is always positive (as far as the hypersurface-orthogonal aether field is concerned) [39]. In addition, there exist both gravitational waves [40–50] and BHs [51–61]. It was also shown that universal horizons can be formed from gravitational collapse of realistic matter [62], in addition to the formation of the spin-0 and metric horizons [63].

In comparison with other modified theories of gravity [64], including scalar-tensor theories and their high-order corrections [65], α -theory has at least two distinguishable features:

- It is a particular vector-tensor theory in which the vector field is always timelike. As a result, it always defines a preferred frame and whereby violates locally the Lorentz invariance (LI). Despite the facts that LI is the cornerstone of modern physics, and all the experiments carried out so far are consistent with it [66–71], violations of LI have been well motivated and extensively studied in the past several decades, especially from the point of view of quantum gravity [72–76].
- BHs in α -theory are defined in terms of universal horizons (UHs) [54], instead of metric horizons (MHs) as that in GR. This is due to the fact that in α -theory there exist three different species of gravitons, spin-0, spin-1, and spin-2, and each of them move in different speeds [77]. To avoid the vacuum gravi-Čerenkov radiation, such as cosmic rays, each of these three species must move with a speed that is at least no less than the speed of light [78]. As a matter of fact, depending on the choice of the free coupling constants of the theory, they can be arbitrarily large, and so far no upper limits of these speeds are known [71].

Clearly, now MHs are no longer one-way membranes to these particles, and they can cross MHs to escape to infinities even initially they are trapped inside them. On the other hand, a UH is defined as the causal boundary of particles with arbitrarily large speeds [54], and once

they are inside it, they can never cross it to escape to spatial infinities (For a recent review of UHs, see, e.g., [76] and references therein).

With the above remarkable features of α -theory, it would be very interesting and important to find new predictions of the theory for the BH spectroscopy [9], the QNMs mentioned above, which has been extensively studied in the last couple of years in terms of GWs emitted in the ringdown phase of binary BHs (BBHs) (for example, see [79–93] and references therein), and found that they are all consistent with GR within the error bars allowed by the observations of the 90 GW events [94].

As the first step to study QNMs in α -theory, recently some of the current authors studied spherically symmetric static spacetimes and obtained various numerical solutions [59], with the choice of the four free parameters involved in the theory that satisfy all the observational constraints [37]¹. We also derived a set of analytic solutions in which the four-parameters satisfy all the self-consistent and observational constraints obtained in [37], and showed that they are nothing but the (anti- or) de Sitter Schwarzschild black holes, in which the aether field are non-trivial but does not contribute to the curvatures of the spacetime. When the cosmological constant vanishes, the universal horizon locates precisely at $r = 3r_s/4$, where r_s denotes the location of the MH.

Lately, we extended our above studies to the stability of such obtained new black holes against odd parity perturbations, and found that they are stable provided that [95],

$$c_4 = 0, \quad (1.1)$$

in addition to the constraint [37],

$$c_{13} \equiv c_1 + c_3 = 0, \quad (1.2)$$

obtained from the observations of GW170817 [96] together with its gamma-ray burst GRB 170817A [97], where c_i 's are the four dimensionless coupling constants of the theory.

In this paper, we continuously study the odd parity perturbations, but focus ourselves on the QNMs of the newly found black holes [59], which, as mentioned above, satisfy all the constraints of the theory [37]. In doing so, several technical questions raise. One of them is connected with the inner boundary conditions, as now the inner boundary is the UH, which is always inside the MH, at which the timelike Killing vector becomes space-like. Then, the notion of “in”- and “out”-going waves must be defined properly, before imposing the condition that there are *no out-going waves* at the UH. In addition, the field equations of perturbations are usually singular

¹ It should be noted that all the solutions obtained previously do not satisfy these conditions, which were the main motivations for us to revisited this problem and obtained new (numerical) solutions in [59].

at the MH, and proper smoothness conditions must be imposed. In GR, the perturbation equations are also singular at MHs, but such smoothness conditions are nicely avoided, as now the MH is the inner boundary, and the smoothness conditions are simply replaced by the inner boundary conditions.

To overcome the above issues, we first choose the ingoing Eddington-Finkelstein (EF) coordinates, so the background is smoothly across the MH, and more important, the ingoing and outgoing waves are well defined over the whole spacetime, including the region between the UH and MH. Then, we carefully study the structure of the field equations near the MH, and find the smoothness conditions that we must impose in order to assure that the field equations hold across the MH. Once the above issues are clarified, we first impose the purely ingoing wave conditions at the UH and purely outgoing wave conditions at the spatial infinity, and then solve the field equations of the odd-parity perturbations by shooting method, respectively, from the UH and the spatial infinity toward the MH. Then, at the MH we impose the smoothness conditions, which are satisfied only for particular choices of the QNM frequency ω , whereby we read off the QNMs of the odd-parity perturbations.

To show the above explicitly, in this paper we shall take the Schwarzschild black hole solution as the background, since it is also a solution of the α -theory [59]. The main reasons in doing are two-folds: i) First, in such a background, the mathematics involved will be much simple, from which we can construct clearly the boundary conditions at UHs and at spatial infinities, as well as the smoothness conditions across MHs. ii) Second, we can understand deeply the nature of the instability of this solution found in [95] from the point of view of QNMs, as in [95] only its stability against large angular perturbations was studied.

Specifically, the paper is organized as follows. In Section II we first provide a brief introduction to α -theory, and then give various definitions of horizons, including the particle, metric and universal horizons, which are important to the studies of QNMs of black holes, because the fact that superluminal motions exist in the theory, and the inner boundaries of black holes now are the universal horizons. In Section III, we consider the odd-parity perturbations, and construct the master equations, respectively, for the metric and aether field perturbations [cf. Eqs.(3.31) and (3.36)]. In Section IV we first work out step by step the boundary conditions for the master equation of the metric perturbations at the universal horizon as well as at the spatial infinity. Then, we find out the smoothness conditions across the metric horizon. Afterwards, combining the Chandrasekhar-Detweiler method [19] with the shooting method (one side is from the UH to the MH, while the other side is from the spatial infinity to the MH [cf. Section IV.D]), we solve the master equation and find that only for particular choices of the mode ω , can the smoothness conditions at the MH be satisfied, whereby various values of ω are

found and given explicitly in Table I for $l = 2, 3, 4, 10$, respectively. We also compare such a spectrum with the corresponding one given in GR, and find that the differences between them cannot be distinguished by current observations of GWs, although it is well within the detectability of the next generation detectors. In Section V, closely following what is done for the metric perturbations in Section IV, we study the aether perturbations and find various modes for the aether field with $l = 2, 10, 100$, given, respectively, in Tables II and III, in which some unstable modes are identified. This strongly indicates the instability of the aether field, and is also consistent with what was found in [95]. However, due to our numerical errors of the current paper, the existence of such unstable modes is not exclusive. In particular, in the metric perturbations presented in Section IV, no such instability is found. The paper is ended with Section VI, in which we derive our main conclusions and present some remarks on the future investigations.

Through out the paper, we shall adopt the unit system so that $c = G_N = 1$, where c is the speed of light while G_N stands for the Newtonian constant. All the Greek letters run from 0 to 3.

II. EINSTEIN-AETHER THEORY

In Einstein-aether theory (α -theory), the fundamental variables of the gravitational sector are [36],

$$(g_{\mu\nu}, u^\mu, \lambda), \quad (2.1)$$

where $g_{\mu\nu}$ is the four-dimension metric of the spacetime with the signature $(-, +, +, +)$, u^μ is the aether field, and λ is a Lagrangian multiplier, which guarantees that the aether field is always timelike and unity. Then, the general action of the theory is given by,

$$S = S_\alpha + S_m, \quad (2.2)$$

where S_m denotes the action of matter, and S_α the gravitational action of the α -theory, given, respectively, by

$$\begin{aligned} S_\alpha = & \frac{1}{16\pi G_\alpha} \int \sqrt{-g} d^4x \left[\mathcal{L}_\alpha(g_{\mu\nu}, u^\alpha, c_i) \right. \\ & \left. + \mathcal{L}_\lambda(g_{\mu\nu}, u^\alpha, \lambda) \right], \\ S_m = & \int \sqrt{-g} d^4x \left[\mathcal{L}_m(g_{\mu\nu}, u^\alpha; \hat{\psi}) \right]. \end{aligned} \quad (2.3)$$

Here $\hat{\psi}$ collectively denotes the matter fields, and g is the determinant of $g_{\mu\nu}$, and

$$\begin{aligned} \mathcal{L}_\lambda & \equiv \lambda \left(g_{\alpha\beta} u^\alpha u^\beta + 1 \right), \\ \mathcal{L}_\alpha & \equiv R(g_{\mu\nu}) - M^{\alpha\beta}{}_{\mu\nu} (D_\alpha u^\mu) (D_\beta u^\nu), \end{aligned} \quad (2.4)$$

where D_μ denotes the covariant derivative with respect to $g_{\mu\nu}$, R is the Ricci scalar, and $M^{\alpha\beta}{}_{\mu\nu}$ is defined as

$$M^{\alpha\beta}{}_{\mu\nu} \equiv c_1 g^{\alpha\beta} g_{\mu\nu} + c_2 \delta_\mu^\alpha \delta_\nu^\beta + c_3 \delta_\nu^\alpha \delta_\mu^\beta - c_4 u^\alpha u^\beta g_{\mu\nu}, \quad (2.5)$$

with $\delta_{\mu\nu}$ representing the Kronecker delta. Note that here we assume that matter fields couple not only to $g_{\mu\nu}$ but also to the aether field u^μ . However, in order to satisfy the severe observational constraints, such a coupling in general is assumed to be absent [36].

The four coupling constants c_i 's are all dimensionless, and G_{ae} is related to the Newtonian constant G_N via the relation [98],

$$G_N = \frac{G_{\text{ae}}}{1 - \frac{1}{2}c_{14}}, \quad (2.6)$$

where $c_{ij} \equiv c_i + c_j$.

The variations of the total action, respectively, with respect to $g_{\mu\nu}$, u^μ and λ yield the field equations,

$$R^{\mu\nu} - \frac{1}{2}g^{\mu\nu}R - S^{\mu\nu} = 8\pi G_{\text{ae}}T^{\mu\nu}, \quad (2.7)$$

$$\mathbb{A}_\mu = 8\pi G_{\text{ae}}T_\mu, \quad (2.8)$$

$$g_{\alpha\beta}u^\alpha u^\beta = -1, \quad (2.9)$$

where $R^{\mu\nu}$ denotes the Ricci tensor, and

$$\begin{aligned} S_{\alpha\beta} &\equiv D_\mu \left[J^\mu_{(\alpha} u_{\beta)} + J_{(\alpha\beta)} u^\mu - u_{(\beta} J_{\alpha)}^\mu \right] \\ &\quad + c_1 \left[(D_\alpha u_\mu) (D_\beta u^\mu) - (D_\mu u_\alpha) (D^\mu u_\beta) \right] \\ &\quad + c_4 a_\alpha a_\beta + \lambda u_\alpha u_\beta - \frac{1}{2} g_{\alpha\beta} J^\delta_\sigma D_\delta u^\sigma, \\ \mathbb{A}_\mu &\equiv D_\alpha J^\alpha_\mu + c_4 a_\alpha D_\mu u^\alpha + \lambda u_\mu, \\ T^{\mu\nu} &\equiv \frac{2}{\sqrt{-g}} \frac{\delta(\sqrt{-g}\mathcal{L}_m)}{\delta g_{\mu\nu}}, \\ T_\mu &\equiv -\frac{1}{\sqrt{-g}} \frac{\delta(\sqrt{-g}\mathcal{L}_m)}{\delta u^\mu}, \end{aligned} \quad (2.10)$$

with

$$J^\alpha_\mu \equiv M^{\alpha\beta}{}_{\mu\nu} D_\beta u^\nu, \quad a^\mu \equiv u^\alpha D_\alpha u^\mu. \quad (2.11)$$

From Eq.(2.8), we find that

$$\lambda = u_\beta D_\alpha J^{\alpha\beta} + c_4 a^2 - 8\pi G_{\text{ae}} T_\alpha u^\alpha, \quad (2.12)$$

where $a^2 \equiv a_\lambda a^\lambda$.

It is easy to show that the Minkowski spacetime is a solution of ae -theory, in which the aether is aligned along the time direction, $\bar{u}_\mu = \delta_\mu^0$. Then, the linear perturbations around the Minkowski background show that the theory in general possess three types of excitations, scalar (spin-0), vector (spin-1) and tensor (spin-2) modes, with their squared speeds given by [77]

$$\begin{aligned} c_S^2 &= \frac{c_{123}(2 - c_{14})}{c_{14}(1 - c_{13})(2 + c_{13} + 3c_2)}, \\ c_V^2 &= \frac{2c_1 - c_{13}(2c_1 - c_{13})}{2c_{14}(1 - c_{13})}, \\ c_T^2 &= \frac{1}{1 - c_{13}}, \end{aligned} \quad (2.13)$$

respectively. Here $c_{ijk} \equiv c_i + c_j + c_k$.

Requiring that the theory: (a) be self-consistent, such as free of ghosts; and (b) satisfies all the observational constraints obtained so far, it was found that the parameter space of the theory is considerably restricted. In particular, c_{14} , c_2 and c_{13} are restricted to [37] ²,

$$0 \lesssim c_{14} \lesssim 2.5 \times 10^{-5}, \quad (2.14)$$

$$c_{14} \lesssim c_2 \lesssim 0.095, \quad (2.15)$$

$$|c_{13}| \lesssim 10^{-15}. \quad (2.16)$$

Finally, the stability of the odd-parity perturbations of BHs further requires $c_4 = 0$ [cf. Eq.(1.1)], provided that the condition $c_{13} = 0$ holds precisely [95].

A. Particle and Universal Horizons

In this subsection, we shall provide a brief review on several horizons, including universal horizons, as they are important to the investigations of the QNMs of black holes in gravitational theories with broken LI. Although they will be reviewed in the framework of the Einstein-aether theory, their generalizations to other theories are straightforward. For more details, we refer readers to [76].

1. Particle Horizons

In particular, the ae -theory possesses three different modes, and all of them are moving in different speeds. In general each of these different modes defines a particle horizon [36]. These horizons are the null surfaces of the effective metrics,

$$g_{\alpha\beta}^{(A)} \equiv g_{\alpha\beta} - (c_A^2 - 1) u_\alpha u_\beta, \quad (2.17)$$

where $A = S, V, T$. The null surfaces for $A = S, V, T$ are called spin-0 horizon (S0H), spin-1 horizon (S1H) and spin-2 horizon (S2H), respectively. These three different horizons will be referred as particle horizons for the corresponding gravitons.

In the spherically symmetric case, the static spacetimes are described by the general metric

$$ds^2 = -F(r)dv^2 + 2B(r)dvdr + r^2 d\Omega^2, \quad (2.18)$$

where $d\Omega^2 \equiv d\theta^2 + \sin^2\theta d\varphi^2$ and $x^\mu = (v, r, \theta, \varphi)$ denote the ingoing EF coordinates. In this system of coordinates, the aether field takes the form

$$u^\alpha \partial_\alpha = A(r) \partial_v - \frac{1 - F(r)A^2(r)}{2B(r)A(r)} \partial_r, \quad (2.19)$$

² The recent studies of the neutron binary systems showed that the PPN parameter α_1 is further restricted to $|\alpha_1| < 10^{-5}$ [50], which is an order of magnitude stronger than the bounds from lunar laser ranging experiments [99]. This will translate the constraint on c_{14} given by Eq.(2.14) to $0 \lesssim c_{14} \lesssim 2.5 \times 10^{-6}$, as one can see clearly from Eq.(3.12) given in [37].

where $A(r)$ is an arbitrary function of r , and will be determined by the Einstein-aether field equations, together with the metric coefficients $F(r)$ and $B(r)$.

Then, the out-going normal vector to the hypersurface $r = r_0$ is given by

$$N_\alpha \equiv \frac{\partial(r - r_0)}{\partial x^\alpha} = \delta_\alpha^r, \quad (2.20)$$

where r_0 is a constant. In terms of N_α , the spin-0, spin-1, and spin-2 horizons are defined, respectively, by

$$g_{\alpha\beta}^{(A)} N^\alpha N^\beta \Big|_{r=r_A} = 0, \quad (2.21)$$

where r_A denotes the location of the horizon of the particle with spin- A .

On the other hand, the MH is the null surface of metric $g_{\alpha\beta}$, or a particle horizon of $g_{\alpha\beta}^{(A)}$ with $c_A = 1$, given by

$$g_{\alpha\beta} N^\alpha N^\beta \Big|_{r=r_{\text{MH}}} = 0. \quad (2.22)$$

2. Universal Horizons

To define the universal horizon, let us first note that, if a BH is defined to be a region that traps all possible causal influences, it must be bounded by a horizon corresponding to the fastest speed. In theories with the broken LI, the dispersion relation of a massive particle contains generically high-order momentum terms [76],

$$E^2 = m^2 + p_k^2 k^2 \left(1 + \sum_{n=1}^{2(z-1)} q_n \left(\frac{k}{M_*} \right)^n \right), \quad (2.23)$$

from which we can see that both of the group and phase velocities become unbounded as $k \rightarrow \infty$, where E and k are the energy and momentum of the particle considered, and p_k and q_n 's are coefficients, depending on the species of the particle, while M_* is the suppression energy scale of the higher-dimensional operators. Therefore, in theories with the broken LI, a BH should be defined to be a region that traps all possible causal influences, including particles with arbitrarily large speeds ($c_A \rightarrow \infty$).

Does such a region exist? To answer this question, let us first note that the causal structure of spacetimes in such theories is quite different from that given in GR, where the light cone at a given point p plays a fundamental role in determining the causal relationship of p to other events [100]. In a ultraviolet (UV) complete theory, the above dispersion relationship is expected even in the gravitational sector³. In such theories, the causal

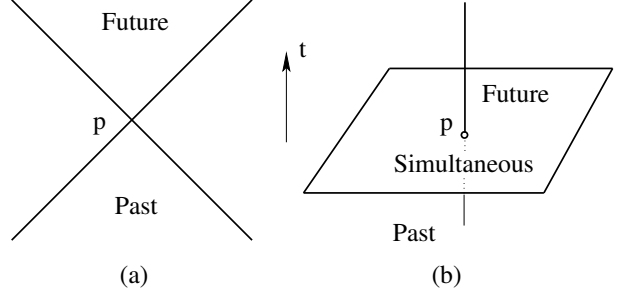


FIG. 1. Illustration of causal structures of spacetimes in different theories of gravity [100]: (a) The light cone of the event p in special relativity. (b) The causal structure of the event p in Newtonian theory.

structure is dramatically changed. For example, in Newtonian theory, time is absolute and the speeds of signals are not limited. Then, the causal structure of a given point p is uniquely determined by the time difference, $\Delta t \equiv t_p - t_q$, between the two events [cf. Fig. 1]. In particular, if $\Delta t > 0$, the event q is to the past of p ; if $\Delta t < 0$, it is to the future; and if $\Delta t = 0$, the two events are simultaneous.

In theories with broken LI, a similar situation occurs. Thus, to consider the causal structure of spacetimes in such theories, a globally time-like “coordinate” needs to be introduced [54] (See also [55]). In particular, for a given spacetime, let us first introduce a globally timelike scalar field $\hat{\phi}$ [104], so that

$$g^{\alpha\beta} \hat{\phi}_{,\alpha} \hat{\phi}_{,\beta} > 0, \quad (2.24)$$

over the whole spacetime. It is interesting to note that, in spherically symmetric spacetimes, the timelike aether field u_μ is hypersurface-orthogonal [76, 105], and can always be expressed as the gradient of a scalar field [106],

$$u_\mu = \frac{\phi_{,\mu}}{\sqrt{-\phi_{,\alpha} \phi^{,\alpha}}}. \quad (2.25)$$

Therefore, now a natural choice is to identify $\hat{\phi}$ with ϕ , $\hat{\phi} = \phi$. Then, similar to Newtonian theory, this field defines globally an absolute time direction: *all particles are assumed to move along the increasing direction of the timelike scalar field ϕ* . It is clear with this definition of the time direction, the causality now is well-defined, quite similar to Newtonian theory [cf. Fig. 2]. With such a definition, one can see that, for a given spacetime there may exist a surface $r = r_{\text{UH}}$, at which the aether field u_μ is orthogonal to the timelike Killing vector [108] ζ ($\equiv \partial_v$),

$$\zeta \cdot u|_{r=r_{\text{UH}}} = -\frac{1}{2A} (1 + J) \Big|_{r=r_{\text{UH}}} = 0, \quad (2.26)$$

where $J \equiv FA^2$ [59]. Given that all particles move along the increasing direction of the aether field, it is clear that

³ One of such examples is the healthy extension [101, 102] of Hořava gravity [76, 103], a possible UV extension of the khronometric theory.

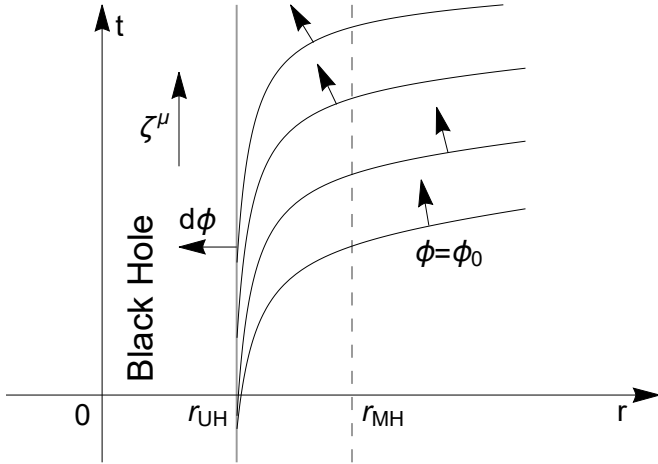


FIG. 2. Illustration of the bending of the $\phi = \text{constant}$ surfaces, and the existence of the UH in a spherically symmetric static spacetime, where ϕ denotes the globally timelike scalar field, and t is the Painlevé-Gullstrand-like coordinates, which covers the whole spacetime [107]. Particles move always along the increasing direction of ϕ . The Killing vector $\zeta^\mu = \delta_v^\mu$ always points upward at each point of the plane. The vertical dashed line is the location of the metric (Killing) horizon, $r = r_{\text{MH}}$. The UH, denoted by the vertical solid line, is located at $r = r_{\text{UH}}$, which is always inside the MH.

a particle must cross this surface and move inward, once it arrives at it, no matter how large its speed is⁴. This is a one-way membrane, and particles even with infinitely large speeds cannot escape from it, once they are inside it. So, it acts as an absolute horizon to all particles (with any speed), which is often called the UH [54, 55, 76].

The extension of the definition of UHs to dynamical spacetimes is given in [62], in which it was shown explicitly that such dynamical UHs can be formed from gravitational collapse of realistic matter fields.

B. The de Sitter-Schwarzschild Black Hole Solutions

When $c_{13} = c_{14} = 0$, there exists a particular class of analytic solutions of the background Einstein-aether field

equations [59],

$$\begin{aligned} F(r) &= F_2 \left(1 - \frac{2m}{r} \right) + \frac{\Lambda}{3} r^2, \\ B &= \sqrt{F_2}, \quad \Lambda \equiv \frac{9}{8} c_2 w_1^2 w_2^2, \\ A(r) &= -\frac{w_2}{2F} \left[\left(\frac{1}{r^2} + w_1 r \right) \right. \\ &\quad \left. \pm \sqrt{\frac{4F}{w_2^2} + \left(\frac{1}{r^2} + w_1 r \right)^2} \right], \end{aligned} \quad (2.27)$$

where F_2 , m , w_1 and w_2 are four integration constants. Using the gauge freedom of the EF coordinates, without loss of the generality, we can always set $F_2 = 1$. Then, the spacetime is precisely the anti-de Sitter or de Sitter Schwarzschild black hole solutions, depending on the signs of the coupling constant c_2 . However, the constraints (2.14) and (2.15) tell us that $c_2 \geq 0$, so it must be the de Sitter Schwarzschild solution, where $r_s = 2m$ is the Schwarzschild radius. In this paper, we shall consider only the case $w_1 = 0$, so that the spacetime is described precisely by the Schwarzschild solution. Then, as $r \rightarrow \infty$, we find that

$$\lim_{r \rightarrow \infty} A(r) = \mp 1, \quad (F_2 = 1, w_1 = 0). \quad (2.28)$$

Thus, we shall choose the “-” sign for the expression of $A(r)$ in Eq.(2.27), so that $\lim_{r \rightarrow \infty} A(r) = +1$, which is also consistent with the asymptotical-flatness conditions adopted in [59]. Then, for a UH to exist, we must set $w_2 = 3\sqrt{3}r_s^2/8$ [108], for which the UH is located at

$$r_{\text{UH}} = \frac{3}{4}r_s. \quad (2.29)$$

Note that in the current case we have

$$c_S = \infty, \quad c_T = c_V = 1, \quad (c_{13} = c_{14} = 0), \quad (2.30)$$

as can be seen from Eq. (2.13), which implies that now the S0H coincides with the UH, while the S1H and S2H coincide with the MH.

It is interesting to note that in this particular case, the aether field has no influence on the spacetime geometry. However, the aether field is non-trivial, and quite different from the one given in the Minkowski spacetime. This will in turn affect the perturbation equations of the Einstein-aether gravity, as to be seen clearly in the next section.

III. ODD-PARITY PERTURBATIONS AND FIELD EQUATIONS

To study the linear perturbations of the spherically symmetric spacetimes in the framework of α -theory, let

⁴ Particles even with infinitely large speeds would just move on these boundaries and cannot escape to infinity.

us first introduce the more familiar Schwarzschild coordinate t via the relation,

$$t = v - f(r), \quad df \equiv \frac{B}{F} dr, \quad (3.1)$$

from which we find that the background metric (2.18) and background aether field (2.19) take the form,

$$d\bar{s}^2 = -F(r)dt^2 + \frac{B^2(r)}{F(r)}dr^2 + r^2d\Omega^2, \quad (3.2)$$

$$\bar{u}^\alpha \partial_\alpha = \frac{FA^2 + 1}{2AF} \partial_t + \frac{FA^2 - 1}{2AB} \partial_r. \quad (3.3)$$

Clearly, this metric becomes singular at the MH, $F(r_s) = 0$, so that the coordinates cannot cover the whole region $r \in (0, \infty)$. However, now the inner boundary is not at the MH, but rather at the UH, which is always inside the MH. Therefore, to impose the boundary conditions at $r = r_{\text{UH}}$ and $r = \infty$ simultaneously, we shall work out the linear perturbations in the EF coordinates, in which the metric takes the form of Eq.(2.18). On the other hand, setting

$$u \equiv t - f(r), \quad (3.4)$$

we find that the metric (3.2) takes the form

$$d\bar{s}^2 = -F(r)du^2 - 2B(r)du dr + r^2d\Omega^2, \quad (3.5)$$

which is the metric written in terms of the out-going EF coordinate u . Although the roles of t and r will be exchanged across a MH, the “in-going” and “out-going”

coordinates v and u remain the same in the whole spacetime. So, in the rest of the paper we always refer the “in-going” and “out-going” in terms of the coordinates v and u .

Once the above issues are clarified, now let us consider the perturbations of the background solutions given by Eq.(2.27) with

$$F_2 = 1, \quad w_1 = 0, \quad w_2 = \frac{3\sqrt{3}r_s^2}{8}. \quad (3.6)$$

For such choices, the background spacetime is precisely the Schwarzschild vacuum solution,

$$F = 1 - \frac{r_s}{r}, \quad B = 1, \quad (3.7)$$

as shown in the last section.

Denoting the background metric and aether field by $\bar{g}_{\mu\nu}$ and \bar{u}_μ , respectively, the total metric and aether field are given by,

$$g_{\mu\nu} = \bar{g}_{\mu\nu} + \epsilon h_{\mu\nu}, \quad u_\mu = \bar{u}_\mu + \epsilon w_\mu, \quad (3.8)$$

where ϵ is a book-marker, and we shall expand the perturbations only to its first order. Later, we can safely set it to one. Then, working in the in-going EF coordinates (v, r, θ, ϕ) , and with only the odd-parity part, we find that the linear perturbations $h_{\mu\nu}$ and w_μ can be cast in the forms [95, 109],

$$h_{\mu\nu} = \sum_{l=0}^{\infty} \sum_{m=-l}^l \begin{pmatrix} 0 & 0 & C_{lm} \csc \theta \partial_\varphi & -C_{lm} \sin \theta \partial_\theta \\ 0 & 0 & J_{lm} \csc \theta \partial_\varphi & -J_{lm} \sin \theta \partial_\theta \\ \text{sym} & \text{sym} & G_{lm} \csc \theta \left(\cot \theta \partial_\varphi - \partial_\theta \partial_\varphi \right) & \text{sym} \\ \text{sym} & \text{sym} & \frac{1}{2} G_{lm} \left(\sin \theta \partial_\theta^2 - \cos \theta \partial_\theta - \csc \theta \partial_\varphi^2 \right) & -G_{lm} \sin \theta \left(\cot \theta \partial_\phi - \partial_\theta \partial_\varphi \right) \end{pmatrix} Y_{lm}(\theta, \varphi), \quad (3.9)$$

and

$$w_\mu = \sum_{l=0}^{\infty} \sum_{m=-l}^l \begin{pmatrix} 0 \\ 0 \\ a_{lm} \csc \theta \partial_\varphi \\ -a_{lm} \sin \theta \partial_\theta \end{pmatrix} Y_{lm}(\theta, \varphi), \quad (3.10)$$

where $Y_{lm}(\theta, \varphi)$ stands for the spherical harmonics, and

C_{lm} , G_{lm} , J_{lm} and a_{lm} are functions of v and r only⁵. Note that when calculating the field equations we will set $m = 0$ in the above expressions so that $\partial_\varphi Y_{lm}(\theta, \varphi) = 0$, as now the background has the spherical symmetry, and the corresponding linear perturbations do not depend on m [109, 110]⁶.

⁵ It must not be confused with the function J_{lm} introduced here and the tensor $J_{\alpha\beta}$ appearing in Eq.(2.10).

⁶ Notice that, since we are using the EF coordinate and following some different conventions, the terms $\{C_{lm}, J_{lm}, G_{lm}\}$ in (3.9) are not necessarily equal to their counterparts given in [109].

A. Gauge Transformations

For later convenience, we first investigate the infinitesimal gauge transformations (Recall that we only consider the odd-parity perturbations and $m = 0$)

$$x^\alpha \rightarrow x'^\alpha = x^\alpha + \epsilon \xi^\alpha, \quad (3.11)$$

where

$$\xi^\alpha = -\frac{\csc \theta \partial_\theta Y_{lm}(\theta, \phi)}{r^2} \{0, 0, 0, 1\} \xi, \quad (3.12)$$

with ξ being a function of v and r . Under the transformation of Eq.(3.11), we have

$$\begin{aligned} \Delta w_\mu &\equiv (w_\mu)_{new} - (w_\mu)_{old} = -\mathcal{L}_\xi \bar{u}_\mu, \\ \Delta h_{\mu\nu} &\equiv (h_{\mu\nu})_{new} - (h_{\mu\nu})_{old} = -\mathcal{L}_\xi \bar{g}_{\mu\nu}, \end{aligned} \quad (3.13)$$

where \mathcal{L} stands for the Lie derivative [111]. From Eq.(3.13) we find

$$\begin{aligned} \Delta C_{lm} &\equiv (C_{lm})_{old} - (C_{lm})_{new} = \dot{\xi}, \\ \Delta G_{lm} &\equiv (G_{lm})_{old} - (G_{lm})_{new} = -2\xi, \\ \Delta J_{lm} &\equiv (J_{lm})_{old} - (J_{lm})_{new} = \xi' - \frac{2}{r}\xi, \\ \Delta a_{lm} &\equiv (a_{lm})_{old} - (a_{lm})_{new} = 0, \end{aligned} \quad (3.14)$$

where a prime and a dot stand for the derivatives with respect to r and v , respectively. With the above gauge transformations, we can construct the gauge-invariant quantities, and due to the presence of the aether field, three such independent quantities can be constructed, in contrast to the relativistic case, in which only two such quantities can be constructed. These three gauge invari-

ants can be defined as

$$\begin{aligned} \mathcal{X}_{lm}(v, r) &\equiv C_{lm} + \frac{1}{2}\dot{G}_{lm}, \\ \mathcal{Y}_{lm}(v, r) &\equiv \frac{2}{r}C_{lm} - C'_{lm} + \dot{J}_{lm}, \\ \mathcal{Z}_{lm}(v, r) &\equiv a_{lm}. \end{aligned} \quad (3.15)$$

Of course, any combination of these quantities is also gauge-invariant. By properly fixing the gauge, the resultant field equations will be simplified considerably. In the current case, we find that one of the most convenient gauge choices is

$$C_{lm} = 0, \quad (3.16)$$

from which we find

$$\xi(v, r) = \int [C_{lm}(v, r)]_{old} dv + \hat{C}_1(r), \quad (3.17)$$

where \hat{C}_1 is an arbitrary function of r . Therefore, with this choice of gauge, we still have the gauge residual

$$\hat{\xi}(v, r) = \hat{C}_1(r). \quad (3.18)$$

We shall come back to this point later, and fix the gauge residual completely by properly imposing an additional gauge condition.

B. Linearized Field Equations

When the spacetimes are in the vacuum, we have $T_{\mu\nu} = 0$, $T_\mu = 0$, and then the field equations (2.7) and (2.8) reduce to

$$E_{\mu\nu} \equiv G_{\mu\nu} - S_{\mu\nu} = 0, \quad (3.19)$$

$$\mathcal{A}^\mu = 0, \quad (3.20)$$

where $G_{\mu\nu} \equiv R_{\mu\nu} - g_{\mu\nu}R/2$. To the first-order of ϵ and with the gauge (3.16), we find that there are only four non-trivial equations, which are given by

$$E_{\phi t} = E_{\phi r} = E_{\phi\theta} = \mathcal{A}^\phi = 0, \quad (3.21)$$

and can be cast respectively in the forms,

$$\rho_{101}\ddot{J}_{lm} + \rho_{102}\dot{J}_{lm} + \rho_{103}\dot{J}'_{lm} + \rho_{104}a_{lm} + \rho_{105}\dot{a}_{lm} + \rho_{106}\ddot{a}_{lm} + \rho_{107}\dot{a}'_{lm} + \rho_{108}\dot{a}_{lm}' + \rho_{109}\dot{a}_{lm}'' + \rho_{110}\dot{G}_{lm} = 0, \quad (3.22)$$

$$\begin{aligned} \rho_{201}J_{lm} + \rho_{202}\dot{J}_{lm} + \rho_{203}\dot{J}'_{lm} + \rho_{204}a_{lm} + \rho_{205}\dot{a}_{lm} + \rho_{206}\ddot{a}_{lm} + \rho_{207}\dot{a}'_{lm} + \rho_{208}\dot{a}_{lm}' + \rho_{209}\dot{a}_{lm}'' + \rho_{210}G_{lm} \\ + \rho_{211}G'_{lm} = 0, \end{aligned} \quad (3.23)$$

$$\rho_{301}J_{lm} + \rho_{302}\dot{J}_{lm} + \rho_{303}\dot{J}'_{lm} + \rho_{304}G_{lm} + \rho_{305}\dot{G}_{lm} + \rho_{306}\dot{G}'_{lm} + \rho_{307}G'_{lm} + \rho_{308}G''_{lm} = 0, \quad (3.24)$$

$$\rho_{401}a_{lm} + \rho_{402}\dot{a}_{lm} + \rho_{403}\ddot{a}_{lm} + \rho_{404}\dot{a}'_{lm} + \rho_{405}\dot{a}_{lm}' + \rho_{406}\dot{a}_{lm}'' = 0. \quad (3.25)$$

It is interesting to note that the coefficients ρ_{abc} are functions of r , c_1 and l only, and some of them contain no

c_1 . Their expressions are given explicitly in Appendix A. More importantly, from Eq. (3.25) we can see clearly

that a_{lm} has been decoupled from J_{lm} and G_{lm} .

C. Master Equations

Since there are only three independent unknowns in Eqs. (3.22)-(3.25), G_{lm} , J_{lm} and a_{lm} , one of the above four equations must not be independent, although this non-dependent equation can still be used to simplify the

derivations of the master equation. To simplify the following discussions, using the rescaling symmetry of the background [59], we first set $r_s = 1$. Then, we have

$$f(r) \equiv \int \frac{B}{F} dr = r + \ln |r - 1|. \quad (3.26)$$

Combining Eqs.(3.22)-(3.25), we obtain the following master equation for the gauge invariant \mathcal{Y}_{lm} ,

$$\left\{ \frac{(r-1)^2}{r^2} \frac{\partial^2}{\partial r^2} + \frac{(r-1)(2r-1)}{r^3} \frac{\partial}{\partial r} + 2 \left(1 - \frac{1}{r}\right) \frac{\partial^2}{\partial r \partial v} + \frac{2(r-1)}{r^2} \frac{\partial}{\partial v} - \frac{(r-1)[l(l+1)r-4]}{r^4} \right\} \mathcal{Y}_{lm} = 0, \quad (3.27)$$

where $\mathcal{Y}_{lm} = \dot{J}_{lm}$ for our current gauge choice (3.16). Setting

$$\mathcal{Y}_{lm}(v, r) = e^{-i\omega v} \bar{\mathcal{Y}}_{lm}(r), \quad (3.28)$$

where ω is the QNM frequency to be calculated below, (3.27) reduces to

$$\left\{ \frac{(r-1)^2}{r^2} \frac{\partial^2}{\partial r^2} + \left[\frac{(r-1)(2r-1)}{r^3} - 2i\omega \left(1 - \frac{1}{r}\right) \right] \frac{\partial}{\partial r} - \frac{2i\omega(r-1)}{r^2} - \frac{(r-1)[l(l+1)r-4]}{r^4} \right\} \bar{\mathcal{Y}}_{lm} = 0. \quad (3.29)$$

To eliminate the first-order derivative term of the above equation, we introduce the function $\Psi(r)$ via the relation,

$$\Psi(r) \equiv e^{-i\omega f(r)} r \bar{\mathcal{Y}}_{lm}(r), \quad (3.30)$$

so that Eq. (3.29) can be cast in the simple form,

$$\left[\frac{d^2}{dx^2} + (\omega^2 - V_g) \right] \Psi = 0, \quad (3.31)$$

where $x \equiv f(r)$ given by Eq.(3.26), and

$$V_g \equiv \frac{(r-1)[l(l+1)r-3]}{r^4}. \quad (3.32)$$

It is interesting to note that V_g is identical to the effective potential given in the Regge-Wheeler equation in GR [29]. However, due to the different locations of the inner boundaries, in general different BH spectroscopies are expected.

On the other hand, the combination of Eqs.(3.22) and (3.25) yields,

$$\begin{aligned} \mathcal{X}_{lm} &= -\frac{1}{(l+2)(l-1)} \\ &\times \left[2(r-1) + r(r-1) \frac{\partial}{\partial r} + r^2 \frac{\partial}{\partial v} \right] \mathcal{Y}_{lm}. \end{aligned} \quad (3.33)$$

Then, from Eq.(3.15) we find

$$G_{lm}(v, r) = 2 \int \mathcal{X}(v, r) dv + \hat{G}_{lm}(r), \quad (3.34)$$

where $\hat{G}_{lm}(r)$ is an arbitrary function of r only. However, using the gauge residual (3.18), we can always set it to zero, by choosing

$$\hat{C}(r) = -\frac{1}{2} \hat{G}_{lm}(r). \quad (3.35)$$

Clearly, with this choice the remaining gauge freedom is completely fixed.

In addition, Eq.(3.25) can be written as

$$\left[\frac{(r-1)^2}{r^2} \frac{d^2}{dr^2} + \frac{r-1}{r^3} \frac{d}{dr} - V_{\text{eff}}(r) \right] \psi = 0, \quad (3.36)$$

where

$$\psi(r) \equiv \sqrt{\frac{r}{r-1}} \exp \left\{ \int \frac{54(1-r) + r \left[128(r-1)r + 3i\sqrt{768(r-1)r^3 + 81}\omega_{\text{ae}} \right]}{(3-4r)^2(r-1)r[8r(2r+1)+3]} dr \right\} \hat{\mathcal{Z}}_{lm}(r), \quad (3.37)$$

$$V_{\text{eff}} \equiv \frac{1}{4(256r^8 - 256r^7 + 27r^4)} \left[1024l(l+1)r^6 - 1024 \left(2l^2 + 2l + 1 \right) r^5 + 256 \left(4l^2 + 4l + 9 \right) r^4 - 1280r^3 + 2160r^2 - 4212r + 2079 \right], \quad (3.38)$$

with

$$a_{lm}(v, r) = e^{-i\omega_{\text{ae}}t} \hat{\mathcal{Z}}_{lm}(r). \quad (3.39)$$

Here t is related to v through Eqs.(3.1) and (3.26). Notice that, a subscript ae is added to ω here to allow it to be different from the QNM spectra ω obtained from Eqs.(3.31) and (3.36).

It is remarkable to note that a_{lm} depends on ω_{ae} only through Eq.(3.37), while Eq.(3.36) shows that ψ itself does not depend on ω_{ae} , although its boundary conditions will depend on ω_{ae} through a_{lm} . We shall come back to this point in the next section.

IV. QNMS OF BLACK HOLES IN EINSTEIN-AETHER THEORY

From the last section, we can see that solving the linearized Einstein-aether field equations for the odd-parity perturbations now reduces to solving the master equations (3.31) and (3.36) with proper boundary conditions. As in GR, they have solutions only for some particular choices of ω and ω_{ae} , which form the spectra of the QNMs of the corresponding BH.

In contrast to GR, due to the existence of superluminal propagations caused by the LI violation, the location of the inner boundary conditions now is moved from MHs to UHs, which are always inside the MHs. There are at least two aspects that make us to believe that QNMs in ae -theory in general deviate from those of GR:

- The different locations of the inner boundaries. It is true that in both theories it is all required that only “in-going” waves be allowed at the inner boundaries. However, when these conditions are imposed at UHs (as required by ae -theory), it is expected that at the corresponding MHs both “in-going” and “out-going” waves exist (which is quite different from that of GR), because of the existence of the superluminal propagations.
- The different dynamical differential equations. Despite the fact that the background in both theories is the same and all described by the Schwarzschild BH, the linearized perturbation equations are different, and in general it is expected that these also alternate the BH QNMs.

With the above in mind, let us turn to consider the initial conditions respectively at the UH ($r = r_{\text{UH}} = 3/4$) and spatial infinity ($r \rightarrow +\infty$). Once these are done, we turn ourselves to consider the smoothness conditions at the MH.

A. Boundary Conditions at the Spatial Infinities

As mentioned above, the boundary conditions at the spatial infinity are that only “out-going” waves exist. To see the implication of these conditions on the gauge-invariant quantities \mathcal{Y}_{lm} and a_{lm} , let us first note that as $r \rightarrow +\infty$, to the leading order, we have $f(r) \simeq r$, and $v \simeq t + r$ and $u \simeq t - r$. Then, Eq.(3.31) has the general solutions,

$$\Psi|_{r \rightarrow \infty} = a_+ e^{i\omega x} + a_- e^{-i\omega x}, \quad (4.1)$$

where a_{\pm} are two integration constants. Inserting the two branches of (4.1) into (3.30), and together with Eq. (3.28), we find that

$$\mathcal{Y}_{lm}(v, r)|_{r \rightarrow +\infty} \propto r a_{\pm} e^{-i\omega(t \mp x)}. \quad (4.2)$$

Therefore, to have only outgoing-waves, we must set $a_- = 0$. As a result, when r is very large, we expect $\Psi(r)$ to take the form,

$$\Psi = e^{i\omega x} \sum_{n=0}^{\infty} \frac{a_n}{r^n}, \quad (4.3)$$

where a_n ’s are constants to be determined with the Frobenius-like method [112]. In particular, inserting the above expression into Eq.(3.31), we find the following recursion relation,

$$\begin{aligned} 2i\omega a_n - & \left[(n-1)(n+2i\omega) - l^2 - i \right] a_{n-1} \\ - & \left(l^2 + l - 2n^2 + 5n + 1 \right) a_{n-2} + (n-4)n a_{n-3} = 0, \end{aligned} \quad (4.4)$$

from which we can write all a_n ’s ($n \geq 1$) in terms of a_0 with $a_n \propto a_0$. Since the function $\Phi(r)$ to be introduced below in Eq.(4.19) does not depend on the amplitude of $\Psi(r)$, without loss of the generality, we can always set $a_0 = 1$.

B. Boundary Conditions at Universal Horizons

On the other hand, as $r \rightarrow r_{\text{UH}}$ ($= 3/4$), we note that Eq. (3.29) can be written as

$$\left[\tilde{W}_g(r) \frac{d^2}{dy^2} + (\omega^2 - \tilde{V}_g) \right] \tilde{\Psi} = 0, \quad (4.5)$$

$$\tilde{\Psi} \equiv \sqrt{\frac{r(1-r)}{\tilde{p}}} e^{-i\omega f} \bar{\mathcal{Y}}_{lm}, \quad \tilde{W}_g \equiv \frac{\eta_1}{\tilde{p}^2}, \quad (4.6)$$

where

$$\begin{aligned} \frac{dr}{dy} \equiv \tilde{p}(r) &= \frac{20(l^2 + l - 4)r + 5(-3l^2 + \sqrt{l^2 + l - 4} - 3l + 12)}{20(l^2 + l - 4)r + 5(-3l^2 + 3\sqrt{l^2 + l - 4} - 3l + 12)}, \\ \tilde{V}_g &\equiv \frac{\tilde{W}_g}{4} \left[2\tilde{p} \frac{d(\tilde{p}' - \tilde{p}\eta_2/\eta_1)}{dr} - \left(\tilde{p}' - \frac{\tilde{p}\eta_2}{\eta_1} \right)^2 \right] + \eta_3, \\ \eta_1 &\equiv \frac{(r-1)^2}{r^2}, \quad \eta_2 \equiv \frac{(r-1)(2r-1)}{r^3}, \quad \eta_3 \equiv -\frac{(r-1)(l^2r + lr - 4)}{r^4}. \end{aligned} \quad (4.7)$$

Thus, as $r \rightarrow r_{\text{UH}}$, we have

$$\frac{d^2 \tilde{\Psi}}{dy^2} + \omega^2 \tilde{\Psi} = 0, \quad (4.8)$$

which leads to

$$\tilde{\Psi}|_{r \rightarrow r_{\text{UH}}} = b_+ e^{+i\omega y} + b_- e^{-i\omega y}, \quad (4.9)$$

with b_{\pm} being arbitrary constants. Combining Eqs. (4.9), (4.7) with Eq. (3.28), we find that

$$\begin{aligned} \mathcal{Y}_{lm}(t, r)|_{r \rightarrow r_{\text{UH}}} &\propto b_{\pm} e^{-i\omega(t \mp r)} \sqrt{\frac{\tilde{p}}{r(1-r)}} \\ &\propto b_{\pm} e^{-i\omega(t \mp r)}. \end{aligned} \quad (4.10)$$

Therefore, to satisfy the pure ingoing-wave conditions, we must set $b_+ = 0$. As a result, when $r \rightarrow r_{\text{UH}}$, we expect $\tilde{\Psi}(r)$ to take the form,

$$\tilde{\Psi} = e^{-i\omega y} \sum_{n=0}^{\infty} b_n \left(r - \frac{3}{4} \right)^n. \quad (4.11)$$

Similar to a_n 's, inserting the above expression into Eq.(4.5) we shall find a recursion relation for b_n 's, and from which we can write all $b_{n \geq 1}$'s in terms of b_0 with $b_n \propto b_0$. Again, because of the introduction of $\Phi(r)$ via Eq.(4.19), the choice of b_0 is irrelevant to $\Phi(r)$, so without loss of the generality, we can also set it to one, $b_0 = 1$.

C. Smoothness Conditions across Metric Horizons

In principle, once the two boundary conditions are given, we can solve the two master equations (3.31) and (3.36) to find out the spectrum of ω (ω_{ee}) for any given l . However, since both of them are singular at the MH, we have to solve them first in the regions $r \in (r_{UH}, 1-\epsilon)$ and $r \in (1+\epsilon, \infty)$ separately, and then match the solutions together across the MH, where $0 < \epsilon \ll 1$ [Notice that ϵ used here must not confused with the ones appearing in Eq.(3.8)].

To find out the proper matching conditions, in the neighborhood of $r = 1$, let us first replace $\bar{\mathcal{Y}}_{lm}$ in Eq. (3.29) by $\hat{\mathcal{Y}}_{lm} \equiv e^{-i\omega f} \bar{\mathcal{Y}}_{lm}$, so that it takes the form,

$$\left\{ \frac{(r-1)^2}{r^2} \frac{d^2}{dr^2} + \frac{(r-1)(2r-1)}{r^3} \frac{d}{dr} + \left[\omega^2 - \frac{(r-1)(l^2r + lr - 4)}{r^4} \right] \right\} \hat{\mathcal{Y}}_{lm}(r) = 0. \quad (4.12)$$

Then, we expand $\hat{\mathcal{Y}}_{lm}(r)$ as

$$\hat{\mathcal{Y}}_{lm}(r) = (r-1)^s \sum_{n=0}^{\infty} d_n (r-1)^n, \quad (4.13)$$

where d_n 's are constants to be determined with the

TABLE I. Values of ω for any given l in α -theory and GR, where we have set $c = G_N = r_{MH} (= r_s) = 1$.

l	α	$\Delta\mathcal{A}$	GR	δf	$\delta\tau$
$l = 2$	$-0.74314 - 0.17787i$	4.76×10^{-34}	$-0.74734 - 0.17792i$	-0.00562	-0.00030
	$-0.67267 - 0.54966i$	4.54×10^{-30}	$-0.69342 - 0.54783i$	-0.02993	0.00334
	$-0.56544 - 0.91304i$	9.38×10^{-27}	$-0.60211 - 0.95656i$	-0.06090	-0.04549
$l = 3$	$-1.19890 - 0.18506i$	1.40×10^{-33}	$-1.19889 - 0.18541i$	0.00001	-0.00189
	$-1.16448 - 0.56037i$	3.69×10^{-30}	$-1.16529 - 0.56260i$	-0.00070	-0.00396
	$-1.07995 - 0.95446i$	3.28×10^{-27}	$-1.10337 - 0.95819i$	-0.02122	-0.00388
$l = 4$	$-1.61838 - 0.18832i$	1.05×10^{-18}	$-1.61836 - 0.18833i$	0.00002	-0.00006
	$-1.59342 - 0.56847i$	1.49×10^{-29}	$-1.59326 - 0.56867i$	0.00010	-0.00034
	$-1.54705 - 0.95738i$	9.75×10^{-25}	$-1.54542 - 0.95982i$	0.00106	-0.00254
$l = 10$	$-3.98329 - 0.57582i$	2.14×10^{-14}	$-3.98329 - 0.57582i$	0.00000	0.00000

Frobenius method. In particular, inserting the above expression into Eq.(4.12), we find two branches of solutions,

given, respectively, by

$$s_{\pm} = \pm i\omega. \quad (4.14)$$

Inserting it together with Eq.(4.13) into Eq.(4.12) we find

$$\begin{aligned} n(n+2i\omega)d_n^+ + & \left[-l^2 - l + 2n^2 + n(-3 + 4i\omega) + 2\omega^2 - 3i\omega + 5 \right] d_{n-1}^+ \\ & + \left[-l^2 - l + n^2 + n(-3 + 2i\omega) + 5\omega^2 - 3i\omega + 2 \right] d_{n-2}^+ + 4\omega^2 d_{n-3}^+ + \omega^2 d_{n-4}^+ = 0, \end{aligned} \quad (4.15)$$

for $s = s_+$, and

$$\begin{aligned} n(n-2i\omega)d_n^+ + & \left[-l^2 - l + 2n^2 + n(-3 - 4i\omega) + 2\omega^2 + 3i\omega + 5 \right] d_{n-1}^+ \\ & + \left[-l^2 - l + n^2 + n(-3 - 2i\omega) + 5\omega^2 + 3i\omega + 2 \right] d_{n-2}^+ + 4\omega^2 d_{n-3}^+ + \omega^2 d_{n-4}^+ = 0, \end{aligned} \quad (4.16)$$

for $s = s_-$. Then, similar to a_n 's given by Eq.(4.4), all these coefficients can be written in terms of d_0^{\pm} . With the same reasons as given for the choice of a_0 and b_0 , without loss of the generality, we can always set $d_0^{\pm} = 1$. Therefore, for any given ω and l , we find the general solution of $\hat{\mathcal{Y}}_{lm}(r)$ in the neighborhood of $r = 1$,

$$\hat{\mathcal{Y}}_{lm}(r) = (r-1)^{s_-} \sum_{n=0}^{\infty} d_n^- (r-1)^n + \mathcal{A}(r-1)^{s_+} \sum_{n=0}^{\infty} d_n^+ (r-1)^n, \quad (4.17)$$

with \mathcal{A} being a complex number, and d_n^{\pm} 's are given by Eqs.(4.15) and (4.15) with $d_0^{\pm} = 1$.

It should be noted that in practice Eqs. (4.3), (4.11) and (4.17) cannot be expanded to infinite orders. Instead, we shall expand them to the orders by imposing

certain tolerances to the numerical errors of our numerical computations, and make sure such orders are high enough, so that our main results and conclusions will remain the same, i.e., the numerical solutions adopt convergent behaviors.

D. Algorithm for Solving Master Equations

To solve Eq.(3.29), following [19] we introduce the mode function $\Phi(r)$ by

$$\hat{\mathcal{Y}}_{lm}(r) = \text{Exp} \left(i \int^r \Phi(r) dr \right), \quad (4.18)$$

or equivalently

$$\Phi(r) = -i \frac{d \ln \hat{\mathcal{Y}}_{lm}}{dr}. \quad (4.19)$$

Then, Eq.(3.29) reduces to

$$\begin{aligned} & \frac{i(r-1)^2}{r^2} \Phi' - \frac{(r-1)^2}{r^2} \Phi^2 + \frac{i(2r^2 - 3r + 1)}{r^3} \Phi \\ & - \frac{(r-1)(l^2r + lr - 4)}{r^4} + \omega^2 = 0. \end{aligned} \quad (4.20)$$

It is remarkable to note that such introduced $\Phi(r)$ does not depend on the amplitudes of $\hat{\mathcal{Y}}_{lm}$ around any of the points $r = \{r_{\pm}, r_{\text{UH}}, r_{\text{max}}\}$, with $r_{\pm} \equiv 1 \pm \epsilon$ ($0 < \epsilon \ll 1$) and r_{max} a positive number to be specified. As a result, we can assign a_0 , b_0 and d_0^{\pm} any values. As mentioned previously, without loss of the generality, we shall set all of them to one.

For our convenience, we further introduce a new variable z by $z \equiv 2r/(r + 3/4)$ in Eq.(4.20). In this way, $r \in [3/4, 1) \cup (1, \infty)$ is mapped to $z \in [1, 8/7) \cup (8/7, 2)$. Therefore, Eq.(4.20) becomes

$$\begin{aligned} & \frac{2i(7z^2 - 22z + 16)^2}{27z^2} \frac{d\Phi}{dz} - \frac{(8 - 7z)^2}{9z^2} \Phi^2 \\ & - \frac{8i(35z^3 - 138z^2 + 168z - 64)}{27z^3} \Phi + \omega^2 \\ & - \frac{16(7z - 8)(z - 2)^2 \left[(3l^2 + 3l + 16)z - 32 \right]}{81z^4} = 0. \end{aligned} \quad (4.21)$$

Thus, we obtain a complex ordinary differential equation (ODE) of the first order, which will be much easier to solve than Eq.(3.29). To solve Eq.(4.21) we use the shooting method. Specifically, for any given l , we integrate Eq.(4.21) as follows:

(i) With a good guess, we first choose a (complex) value of ω . Then, by using the polynomial solution (4.11), we create the “initial value” $\tilde{\Psi}_{\text{UH}}(\omega) \equiv \tilde{\Psi}(r = r_{\text{UH}}, \omega)$. After that, we calculate $\Phi_{\text{UH}}(\omega) \equiv \Phi(z = z_{\text{UH}}, \omega)$ using Eq.(4.19), with $z_{\text{UH}} = 2r_{\text{UH}}/(r_{\text{UH}} + 3/4)$.

(ii) With the same ω , using the polynomial solution (4.3), we create the “initial value” $\Psi_{\text{max}}(\omega) \equiv \Psi(r = r_{\text{max}}, \omega)$. After that, we calculate $\Phi_{\text{max}}(\omega) \equiv \Phi(z = z_{\text{max}}, \omega)$ using Eq.(4.19), with $z_{\text{max}} = 2r_{\text{max}}/(r_{\text{max}} + 3/4)$. Here r_{max} is chosen to be sufficiently large.

(iii) By using the initial value $\Phi_{\text{UH}}(\omega)$, integrate Eq.(4.21) from z_{UH} to $z_- = r_-/(r_- + 3/4)$ to obtain $\Phi_- \equiv \Phi(z_-)$. Equalizing this Φ_- and its counterpart given by the polynomial (4.17), we can solve for the combination coefficient \mathcal{A}_- to be denoted by \mathcal{A}_- .

(iv) By using the initial value $\Phi_{\text{max}}(\omega)$, integrate Eq.(4.21) from z_{max} to $z_+ = r_+/(r_+ + 3/4)$ to obtain $\Phi_+ \equiv \Phi(z_+)$. Equalizing this Φ_+ and its counterpart given by the polynomial (4.17), we can again solve for a combination coefficient \mathcal{A}_+ to be denoted by \mathcal{A}_+ .

(v) Logically repeat steps (i)~(iv) to search for the desired ω , with which we have $\Delta\mathcal{A} \equiv |\mathcal{A}_- - \mathcal{A}_+| \lesssim \epsilon_{\text{max}}$, where ϵ_{max} represents our tolerance to the uncertainty.

Note that these iterations could be executed automatically by using *Mathematica*.

E. Numerical Results

Using the algorithm introduced in last subsection, we can obtain various ω for any given l , and some of which are shown in Table I. In this table we also provide the corresponding results from GR (see, e.g., [113]). Comparing the results from α -theory and GR, we can find the differences between these two theories. To characterize these discrepancies, let’s define [8, 114]

$$\begin{aligned} \delta f & \equiv \frac{Re(\omega^{\alpha})}{Re(\omega^{\text{GR}})} - 1, \\ \delta\tau & \equiv \frac{Im(\omega^{\text{GR}})}{Im(\omega^{\alpha})} - 1, \end{aligned} \quad (4.22)$$

which are also given for different modes in Table I. Using the current data provided by the LVK scientific collaboration [94, 114], we are not able to impose any further constraints on α -theory. For instance, combining the results from [94, 114], we find that the most stringent constraint on δf is about $\delta f \approx 0.02 \pm 0.04$. However, the largest discrepancy that we have presented in Table I is still smaller than this limit. Nonetheless, such discrepancies should be well within the detectability of LISA, TianQin and Taiji. In particular, according to Table II provided in [14], the sensitivity of LISA and TianQin to, e.g., δf , could reach about $\mathcal{O}(10^{-5})$. Therefore, they are very likely to be able to distinguish the results from the α -theory and GR, as listed in Table I.

V. INSTABILITY OF THE AETHER FIELD

In the last section, we consider the metric perturbations only, represented by the master equation (3.29). In this section, we turn to study the aether perturbations given by Eqs.(3.36) - (3.39). To this goal, inserting Eq.(3.39) into Eq.(3.25) we obtain

$$\left\{ \kappa_1 \frac{d^2}{dr^2} + \kappa_2 \frac{d}{dr} + \kappa_3 \right\} \hat{\mathcal{Z}}_{lm} = 0, \quad (5.1)$$

where $\kappa_{1,2,3}$ are given in Appendix A. Note that (5.1) is at the same position as (4.12). To solve it, following what we did in the last section, we first specify its boundary conditions at the universal horizon and spatial infinity, as well as the smoothness conditions across the metric horizon, and then solve it with such conditions by the shooting method, one side from the UH to the MH, and the other side from r_{max} to the MH.

A. Boundary Conditions at the Universal Horizon and Spatial Infinity

To find the proper boundary conditions for $\hat{\mathcal{Z}}_{lm}(r)$ at $r \rightarrow 3/4$ and $r \rightarrow +\infty$, we first note that in terms of x Eq.(3.36) takes the form,

$$\left[\frac{d^2}{dx^2} - V_{\text{eff}}(r) \right] \psi = 0. \quad (5.2)$$

Note that (5.2) is at the same position as (3.31).

1. At Spatial Infinity

When $r \rightarrow +\infty$, (5.2) leads to $\psi = \bar{a}_+ + \bar{a}_- x$. For $\hat{\mathcal{Z}}_{lm}$ to be finite at $r \rightarrow +\infty$, we shall set $\bar{a}_- = 0$ [cf. (3.37)]. Thus, we have

$$\psi = \sum_{n=2}^{\infty} \frac{\bar{a}_n}{r^n}, \quad (5.3)$$

where \bar{a}_n can be calculated through recursion relations similar to (4.4). Note that it is known *a posteriori* that the polynomial solution of ψ at $r \rightarrow +\infty$ starts from $n = 2$, as already indicated in Eq.(5.3). Combining with (3.37), we have found the polynomial solution of $\hat{\mathcal{Z}}_{lm}$ in the neighborhood of $r \rightarrow +\infty$.

2. At the Universal Horizon

On the other hand, at the UH, $r = 3/4$, we can write (5.1) in the form,

$$\left[\bar{W}_g(r) \frac{d^2}{d\bar{y}^2} + (-\bar{V}_g) \right] \bar{\psi} = 0, \quad (5.4)$$

where $\bar{W}_g \equiv \kappa_1/\bar{p}^2$, and

$$\begin{aligned} \bar{\psi} &\equiv -\hat{\mathcal{Z}}_{lm} \frac{\sqrt{(64r^3 - 16r^2 - 12r - 9)(2\sqrt{2l^2 + 2l + 9} + 4r - 3)}}{r^2} \\ &\times \exp \left\{ \frac{1}{8} i\omega \left[3\sqrt{6} \tanh^{-1} \left(\frac{8r + 3}{3\sqrt{8r^2 + 4r + \frac{3}{2}}} \right) - 8 \tanh^{-1} \left(\frac{20r + 7}{3\sqrt{24r(2r + 1) + 9}} \right) \right] \right\}, \\ \frac{dr}{d\bar{y}} &\equiv \bar{p}(r) = \frac{4r - 3}{2\sqrt{2l^2 + 2l + 9} + 4r - 3}, \\ \bar{V}_g &\equiv \frac{\bar{W}_g}{4} \left[2\bar{p} \frac{d(\bar{p}' - \bar{p}\kappa_2/\kappa_1)}{dr} - \left(\bar{p}' - \frac{\bar{p}\kappa_2}{\kappa_1} \right)^2 \right] + \kappa_3. \end{aligned} \quad (5.5)$$

When $r \rightarrow (3/4)^+$, (5.4) leads to $\bar{\psi} = \bar{b}_+ e^{+\bar{y}} + \bar{b}_- e^{-\bar{y}}$. For $\hat{\mathcal{Z}}_{lm}$ to be finite at $r \rightarrow (3/4)^+$, we shall set $\bar{b}_- = 0$ [cf. (3.37)]. Thus, we have

$$\bar{\psi} = e^{\bar{y}} \sum_{n=0}^{\infty} \bar{b}_n \left(r - \frac{3}{4} \right)^n. \quad (5.6)$$

Combining with (3.37), we have found the polynomial solution of $\hat{\mathcal{Z}}_{lm}$ in the neighborhood of $r \rightarrow (3/4)^+$.

B. Smoothness Conditions Across the Metric Horizon

At the MH ($r = 1$), it is clear that Eq.(5.1) becomes singular. By following the same procedures of solving

Eq.(4.12), we can also solve Eq.(5.1) in the neighborhood of $r = 1$. To do so, we shall first write $\hat{\mathcal{Z}}_{lm}(r)$ in the form,

$$\hat{\mathcal{Z}}_{lm}(r) = (r - 1)^{\bar{s}} \sum_{n=0}^{\infty} \bar{d}_n (r - 1)^n. \quad (5.7)$$

Just like how we obtain (4.17), the solution is determined to be of the form

$$\hat{\mathcal{Z}}_{lm}(r) = (r-1)^{-i\omega} \left[(r-1) \sum_{n=0}^{\infty} \bar{d}_n^- (r-1)^n + \mathcal{B} \sum_{n=0}^{\infty} \bar{d}_n^+ (r-1)^n \right], \quad (5.8)$$

TABLE II. Values of ω_{ae} by solving Eq.(5.10) for the aether field with $l = 100$ and the units $c = G_N = r_{MH} = 1$.

ω_{ae}	$\Delta\mathcal{B}$
$-1944.19 + 87.4996i$	1.16×10^{-5}
$-2913.80 + 155.310i$	5.19×10^{-6}
$-9886.49 + 267.356i$	4.52×10^{-7}
$-139279.4 + 101836.6i$	1.13×10^{-8}
$-264002.5 + 102057.4i$	5.43×10^{-9}

where \bar{d}_n^{\pm} can be calculated through recursion relations similar to (4.15) and (4.16), and the (complex) constant \mathcal{B} is acting as \mathcal{A} in (4.17).

C. Numerically Solving the aether Master Equation

To solve the aether master equation, let us first set

$$\hat{\mathcal{Z}}_{lm}(r) = \text{Exp} \left(i \int^r \phi(r) dr \right), \quad (5.9)$$

[It must not be confused with ϕ introduced here and the one appearing in Eq.(2.24)] so that Eq.(5.1) takes the form,

$$\alpha_1 \phi'(r) + \alpha_2 \phi(r)^2 + \alpha_3 \phi(r) + \alpha_4 = 0, \quad (5.10)$$

where α_n 's are given in Eq.(A. 7) and must not be confused with the PPN parameters mentioned in Sec. II). With the above given boundary conditions at the universal horizon and spatial infinity, as well as the smoothness conditions across the metric horizon, following the steps presented in Sec. IV.D, we can solve Eq.(5.10) with the shooting method.

However, different from what we have done in Sec. IV, in this section we would like to address the problem of instability found in [95] for large l . In particular, in Table II we present the values of ω_{ae} for $l = 100$. In contrast to those given in Table I, now the imaginary parts of ω_{ae} 's are all positive, which indicates the instability of the aether field. However, we must note the differences between the tolerance levels of Table I indicated by $\Delta\mathcal{A}$ and the ones given in Table II, indicated by $\Delta\mathcal{B}$. In particular, the tolerance levels given by $\Delta\mathcal{B}$ are much weaker than those given by $\Delta\mathcal{A}$.

TABLE III. Values of ω by solving Eq.(5.10) for the aether field with the units $c = G_N = r_{MH} = 1$ for $l = 2, 10$, respectively.

l	ω_{ae}	$\Delta\mathcal{B}$
2	$-43880 \pm 165.44i$	$\mathcal{O}(10^{-11})$
10	$-46071 \pm 291.48i$	$\mathcal{O}(10^{-10})$

In Table III, we also consider the cases $l = 2, 10$, from which it can be seen that unstable modes in each case are also identified, again with much weaker tolerance levels $\Delta\mathcal{B} \approx \mathcal{O}(10^{-10})$.

VI. CONCLUSIONS

In this paper, we have investigated QNMs of black holes in Einstein-aether (æ-) theory, in which the gravitational sector of the theory is described by three different species of gravitons with spins 0, 1, 2, respectively [35]. By properly choosing the four free dimensionless coupling constants, c_i 's, the theory is self-consistent, such as free of ghosts and kinetic instability [36], and satisfies all the observations carried out so far [37, 50, 95]. However, to avoid the vacuum gravi-Čerenkov radiation, such as cosmic rays, each of these three species must move with a speed that is at least no less than the speed of light [78].

Due to the existence of such superluminal motions, we expect that black holes in æ-theory will be dramatically different from those in GR. In particular, the metric horizon that is used to define the boundary of a black hole in GR is no longer a one-way membrane, and particles with superluminal speeds can escape to the spatial infinity, even they are initially trapped inside the metric horizon. As a result, the inner boundary of a black hole now is defined by the universal horizon, a one-way membrane for particles with any speeds, including the ones with infinitely large ones [54]. This in turn implies that at the metric horizon now both “in-going” and “out-going” radiations are expected to exist, which will alternate the QNM spectra of black holes.

In addition, due to the presence of the aether field, the uniqueness theorem of the Schwarzschild black hole does not hold any longer [36], and various black holes in æ-theory exist [59], which can be still formed from gravitational collapse of realistic matter [63], including the formation of universal horizons [62].

The change of the location of a black hole inner boundary from the metric horizon to the universal horizon also results in several technical challenges in the studies of QNMs of black holes. First, the notion of “in-going” and “out-going” radiations must be defined properly, as now the universal horizon is always inside the metric horizon, in which the Schwarzschild timelike coordinate becomes spacelike. In addition, across the metric horizon, the perturbation equations are singular, and proper smoothness conditions must be imposed, too, before solving the corresponding boundary conditions imposed at the universal horizon and the spatial infinity. In GR, the field equations of perturbations are also singular at a metric horizon, but the problem is nicely avoided, as now it is the inner boundary, and the smoothness conditions are simply replaced by the inner boundary conditions.

To overcome the above problems, in this paper we have studied the QNMs of the Schwarzschild black hole, which is also a solution of the Einstein-aether theory [59], in which the presence of the aether field has no effects on the spacetime, although the aether field is non-trivial [cf. Eqs.(2.27) and (3.6)]. Despite the fact that the background is the same as that in GR, it is expected that the corresponding QNMs are different, as now the inner boundary is moved to the universal horizon, and both “in-going” and “out-going” radiations exist at the metric horizon. In addition, the perturbation equations are also different [cf. Eqs.(3.25) and (3.27)].

In particular, in Section III we have constructed the two master equations (3.31) and (3.36), respectively, for the metric and aether field perturbations, while in Section IV we have first worked out step by step the boundary conditions for the master equation of the metric perturbations at the universal horizon, $r_{UH} = 3r_s/4$, where $r_s = 2m$ is the location of the metric horizon, and at the spatial infinity. Then, we have systematically worked out its smoothness conditions across the metric horizon. Afterwards, combining the Chandrasekhar-Detweiler method [19] with the shooting one, one side is from the universal horizon to the metric horizon, while the other side is from the spatial infinity to the metric horizon [cf. Section IV.D], we have found various modes ω for $l = 2, 3, 4, 10$, given explicitly in Table I. In the same table we have also presented the corresponding values of the modes in GR, and found that the differences between

the ones given in α -theory and those given in GR cannot be distinguished by current observations of gravitational waves, although it is well within the detectability of the detectors of the next generation.

In Section V, following closely what we have done for the metric perturbations in Section IV, we have considered the aether perturbations and found various modes ω_α [cf. Eq.(3.39)] for $l = 2, 10, 100$, given, respectively in Tables II and III. In these two tables, in contrast to Table I, we have identified several modes of ω_α ’s, which all have a positive imaginary part. This strongly indicates the instability of the aether field. This is also consistent with what was found in [95] for the Schwarzschild black hole against large angular perturbations. However, due to our numerical errors of the current paper, it must be noted that such a conclusion is not exclusive. In particular, in the metric perturbations presented in Section IV, we have not been able to find such an instability.

Therefore, it would be very important to confirm the above instability and meanwhile extend the current studies to other black holes found in [59]. We wish to report our such studies soon in another occasion.

ACKNOWLEDGMENTS

We would like to express our gratitude to Prof. Shinji Tsujikawa for his valuable comments and suggestions, and to Dr. Xiang Zhao for the early stage of his collaboration of this project. This work is supported in part by the National Key Research and Development Program of China Grant No. 2020YFC2201503, the National Natural Science Foundation of China under Grant No. 11675143 and No. 11975203, the Zhejiang Provincial Natural Science Foundation of China under Grant No. LR21A050001 and LY20A050002, and the Fundamental Research Funds for the Provincial Universities of Zhejiang in China under Grant No. RF-A2019015.

APPENDIX A: THE COEFFICIENTS OF ρ_{abc} , κ_n AND α_m

The coefficients ρ_{abc} appearing in Eqs.(3.22) - (3.25) are given by

$$\begin{aligned}
\rho_{101} &= -\frac{1}{2}, \\
\rho_{102} &= \frac{1-r}{r^2}, \\
\rho_{103} &= \frac{1}{2} \left(\frac{1}{r} - 1 \right), \\
\rho_{104} &= \left\{ 256r^8 \left(16r^2 + 8r + 3 \right) \sqrt{256(r-1)r^3 + 27} \left[\sqrt{256(r-1)r^3 + 27} - 3\sqrt{3} \right]^5 \right\}^{-1} \\
&\quad \times \left\{ c_1 \left[98304\sqrt{3}r^8 - 196608\sqrt{3}r^7 + 98304\sqrt{3}r^6 + 31104\sqrt{3}r^4 - 31104\sqrt{3}r^3 + 6912\sqrt{256(r-1)r^3 + 27}r^3 \right. \right. \\
&\quad \left. \left. - 729\sqrt{256(r-1)r^3 + 27} - 8192\sqrt{256(r-1)r^3 + 27}r^8 + 16384\sqrt{256(r-1)r^3 + 27}r^7 \right. \right. \\
&\quad \left. \left. - 8192\sqrt{256(r-1)r^3 + 27}r^6 - 6912\sqrt{256(r-1)r^3 + 27}r^4 + 2187\sqrt{3} \right] \right. \\
&\quad \times \left[-256r^4 + 256r^3 + 3\sqrt{768(r-1)r^3 + 81} - 27 \right] \\
&\quad \times \left[1024 \left(l^2 + l - 2 \right) r^5 + 128 \left(3l^2 + 3l - 4 \right) r^4 + 2048l(l+1)r^6 + 384r^3 + 3024r^2 + 1512r + 567 \right] \right\}, \\
\rho_{105} &= -\frac{c_1 \left[3\sqrt{3} - \sqrt{256(r-1)r^3 + 27} \right] \left[-256r^4 + 256r^3 + 3\sqrt{768(r-1)r^3 + 81} - 27 \right]}{4096(r-1)^2r^4}, \\
\rho_{106} &= \frac{3c_1(4r-3) \left[\sqrt{768(r-1)r^3 + 81} - 9 \right] \left[-256r^4 + 256r^3 + 3\sqrt{768(r-1)r^3 + 81} - 27 \right]}{8192(r-1)^2r^6\sqrt{256(r-1)r^3 + 27}}, \\
\rho_{107} &= \frac{c_1 \left[256r^4 - 256r^3 - 3\sqrt{768(r-1)r^3 + 81} + 27 \right]^2}{2048(r-1)r^5 \left[3\sqrt{3} - \sqrt{256(r-1)r^3 + 27} \right]}, \\
\rho_{108} &= \left\{ 512r^7 \sqrt{256(r-1)r^3 + 27} \left[\sqrt{256(r-1)r^3 + 27} - 3\sqrt{3} \right]^4 \right\}^{-1} \\
&\quad \times c_1 \left(64r^3 - 27 \right) \left[256r^4 - 256r^3 - 3\sqrt{768(r-1)r^3 + 81} + 27 \right]^2 \\
&\quad \times \left[-128r^4 + 128r^3 + 3\sqrt{768(r-1)r^3 + 81} - 27 \right], \\
\rho_{109} &= -\frac{c_1 \left[-256r^4 + 256r^3 + 3\sqrt{768(r-1)r^3 + 81} - 27 \right]^3}{4096r^6 \left[3\sqrt{3} - \sqrt{256(r-1)r^3 + 27} \right]^3}, \\
\rho_{110} &= -\frac{l^2 + l - 2}{4r^2}, \tag{A. 1}
\end{aligned}$$

$$\begin{aligned}
\rho_{201} &= -\frac{l^2 + l - 2}{2r^2}, \\
\rho_{202} &= \frac{1}{r}, \\
\rho_{203} &= \frac{1}{2}, \\
\rho_{204} &= \left\{ 256(r-1)r^7 \left(16r^2 + 8r + 3 \right) \sqrt{256(r-1)r^3 + 27} \left[\sqrt{256(r-1)r^3 + 27} - 3\sqrt{3} \right]^3 \right\}^{-1} \\
&\quad \times c_1 \left[98304\sqrt{3}r^8 - 196608\sqrt{3}r^7 + 98304\sqrt{3}r^6 + 31104\sqrt{3}r^4 - 31104\sqrt{3}r^3 + 6912\sqrt{256(r-1)r^3 + 27}r^3 \right. \\
&\quad \left. - 729\sqrt{256(r-1)r^3 + 27} - 8192\sqrt{256(r-1)r^3 + 27}r^8 + 16384\sqrt{256(r-1)r^3 + 27}r^7 \right. \\
&\quad \left. - 8192\sqrt{256(r-1)r^3 + 27}r^6 - 6912\sqrt{256(r-1)r^3 + 27}r^4 + 2187\sqrt{3} \right] \\
&\quad \times \left[1024 \left(l^2 + l - 2 \right) r^5 + 128 \left(3l^2 + 3l - 4 \right) r^4 + 2048l(l+1)r^6 + 384r^3 + 3024r^2 + 1512r + 567 \right], \\
\rho_{205} &= -\frac{c_1 \left[3\sqrt{3} - \sqrt{256(r-1)r^3 + 27} \right]^3}{4096(r-1)^3r^3}, \\
\rho_{206} &= \frac{3c_1(4r-3) \left[\sqrt{256(r-1)r^3 + 27} - 3\sqrt{3} \right]^2 \left[\sqrt{768(r-1)r^3 + 81} - 9 \right]}{8192(r-1)^3r^5\sqrt{256(r-1)r^3 + 27}}, \\
\rho_{207} &= \frac{c_1 \left[3\sqrt{3} - \sqrt{256(r-1)r^3 + 27} \right] \left[-256r^4 + 256r^3 + 3\sqrt{768(r-1)r^3 + 81} - 27 \right]}{2048(r-1)^2r^4}, \\
\rho_{208} &= \frac{c_1 \left(64r^3 - 27 \right) \left(256r^4 - 256r^3 - 3\sqrt{768r^4 - 768r^3 + 81} + 27 \right)}{1024(r-1)r^6\sqrt{256r^4 - 256r^3 + 27}}, \\
\rho_{209} &= -\frac{c_1 \left[256r^4 - 256r^3 - 3\sqrt{768(r-1)r^3 + 81} + 27 \right]^2}{4096(r-1)r^5 \left[3\sqrt{3} - \sqrt{256(r-1)r^3 + 27} \right]}, \\
\rho_{210} &= \frac{l^2 + l - 2}{2r^3}, \\
\rho_{211} &= -\frac{l^2 + l - 2}{4r^2}, \tag{A. 2}
\end{aligned}$$

$$\begin{aligned}
\rho_{301} &= \frac{1}{2r^2}, \\
\rho_{302} &= \frac{1}{2}, \\
\rho_{303} &= \frac{r-1}{2r}, \\
\rho_{304} &= \frac{r-2}{2r^3}, \\
\rho_{305} &= -\frac{1}{2r}, \\
\rho_{306} &= \frac{1}{2}, \\
\rho_{307} &= \frac{3-2r}{4r^2}, \\
\rho_{308} &= -\frac{r-1}{4r}, \tag{A. 3}
\end{aligned}$$

$$\begin{aligned}
\rho_{401} &= \left\{ 16r^8 \left(16r^2 + 8r + 3 \right) \sqrt{256(r-1)r^3 + 27} \left[\sqrt{256(r-1)r^3 + 27} - 3\sqrt{3} \right]^4 \right\}^{-1} \\
&\quad \times \left\{ \left[-98304\sqrt{3}r^8 + 196608\sqrt{3}r^7 - 98304\sqrt{3}r^6 - 31104\sqrt{3}r^4 + 31104\sqrt{3}r^3 - 6912\sqrt{256(r-1)r^3 + 27}r^3 \right. \right. \\
&\quad + 729\sqrt{256(r-1)r^3 + 27} + 8192\sqrt{256(r-1)r^3 + 27}r^8 - 16384\sqrt{256(r-1)r^3 + 27}r^7 \\
&\quad \left. \left. + 8192\sqrt{256(r-1)r^3 + 27}r^6 + 6912\sqrt{256(r-1)r^3 + 27}r^4 - 2187\sqrt{3} \right] \right. \\
&\quad \times \left[1024 \left(l^2 + l - 2 \right) r^5 + 128 \left(3l^2 + 3l - 4 \right) r^4 + 2048l(l+1)r^6 + 384r^3 + 3024r^2 + 1512r + 567 \right] \left. \right\}, \\
\rho_{402} &= -\frac{\left(\sqrt{256(r-1)r^3 + 27} - 3\sqrt{3} \right)^2}{256(r-1)^2r^4}, \\
\rho_{403} &= -\frac{3(4r-3) \left[\sqrt{256(r-1)r^3 + 27} - 3\sqrt{3} \right] \left[\sqrt{768(r-1)r^3 + 81} - 9 \right]}{512(r-1)^2r^6\sqrt{256(r-1)r^3 + 27}}, \\
\rho_{404} &= \frac{-256r^4 + 256r^3 + 3 \left(\sqrt{768r^4 - 768r^3 + 81} - 9 \right)}{128(r-1)r^5}, \\
\rho_{405} &= -\frac{\left(64r^3 - 27 \right) \left[128r^4 - 128r^3 - 3\sqrt{768(r-1)r^3 + 81} + 27 \right] \left[256r^4 - 256r^3 - 3\sqrt{768(r-1)r^3 + 81} + 27 \right]}{32r^7\sqrt{256(r-1)r^3 + 27} \left(\sqrt{256(r-1)r^3 + 27} - 3\sqrt{3} \right)^3}, \\
\rho_{406} &= -\frac{27}{256r^6} + \frac{1}{r^3} - \frac{1}{r^2}. \tag{A. 4}
\end{aligned}$$

The coefficients κ_n appearing in Eq.(5.1) are given by

$$\begin{aligned}
\kappa_0 &\equiv \sqrt{256(r-1)r^3 + 27}, \\
\kappa_1 &\equiv \frac{(r-1)^2}{r^2}, \\
\kappa_2 &\equiv \left[4194304r^{14} - 9437184r^{13} + 5505024r^{12} - 65536r^{11} + 2916 \left(\sqrt{768(r-1)r^3 + 81} - 9 \right) r^3 \right. \\
&\quad - 49152 \left(3\sqrt{768(r-1)r^3 + 81} - 53 \right) r^{10} + 36864 \left(5\sqrt{768(r-1)r^3 + 81} - 91 \right) r^9 \\
&\quad - 9216 \left(\sqrt{768(r-1)r^3 + 81} - 15 \right) r^8 - 6912 \left(\sqrt{768(r-1)r^3 + 81} - 15 \right) r^7 \\
&\quad - 41472 \left(\sqrt{768(r-1)r^3 + 81} - 12 \right) r^6 + 5184 \left(\sqrt{768(r-1)r^3 + 81} - 9 \right) r^5 \\
&\quad \left. + 3888 \left(\sqrt{768(r-1)r^3 + 81} - 9 \right) r^4 \right]^{-1} \\
&\quad \times \left\{ \left[4194304r^{12} - 13631488r^{11} + 14942208r^{10} - 7340032r^9 + 15552 \left(7\sqrt{768(r-1)r^3 + 81} - 95 \right) r^3 \right. \right. \\
&\quad + 7776 \left(\sqrt{768(r-1)r^3 + 81} - 9 \right) r - 11664 \left(\sqrt{768(r-1)r^3 + 81} - 9 \right) \\
&\quad - 16384 \left(9\sqrt{768(r-1)r^3 + 81} - 487 \right) r^8 + 12288 \left(27\sqrt{768(r-1)r^3 + 81} - 917 \right) r^7 \\
&\quad - 9216 \left(21\sqrt{768(r-1)r^3 + 81} - 571 \right) r^6 + 64512 \left(\sqrt{768(r-1)r^3 + 81} - 15 \right) r^5 \\
&\quad - 6912 \left(23\sqrt{768(r-1)r^3 + 81} - 327 \right) r^4 - 1296 \left(\sqrt{768(r-1)r^3 + 81} - 9 \right) r^2 \left. \right] \\
&\quad + \left[1944i \left(\sqrt{768(r-1)r^3 + 81} - 9 \right) r^3 + 98304i \left(\sqrt{768(r-1)r^3 + 81} - 27 \right) r^{10} \right. \\
&\quad - 221184i \left(\sqrt{768(r-1)r^3 + 81} - 27 \right) r^9 + 129024i \left(\sqrt{768(r-1)r^3 + 81} - 27 \right) r^8 \\
&\quad - 1536i \left(\sqrt{768(r-1)r^3 + 81} - 27 \right) r^7 + 4608i \left(11\sqrt{768(r-1)r^3 + 81} - 135 \right) r^6 \\
&\quad - 3456i \left(19\sqrt{768(r-1)r^3 + 81} - 243 \right) r^5 + 2592i \left(\sqrt{768(r-1)r^3 + 81} - 9 \right) r^4 \\
&\quad \left. \left. + 5832i \left(\sqrt{768(r-1)r^3 + 81} - 9 \right) r^2 \right] \omega_{\text{ae}} \right\}, \tag{A. 5}
\end{aligned}$$

$$\begin{aligned}
\kappa_3 \equiv & \left[-268435456 \left(12\sqrt{3} - \sqrt{256(r-1)r^3 + 27} \right) r^{18} + 671088640 \left(12\sqrt{3} - \sqrt{256(r-1)r^3 + 27} \right) r^{17} \right. \\
& - 452984832 \left(12\sqrt{3} - \sqrt{256(r-1)r^3 + 27} \right) r^{16} + 16777216 \left(12\sqrt{3} - \sqrt{256(r-1)r^3 + 27} \right) r^{15} \\
& - 1048576 \left(1488\sqrt{3} - 259\sqrt{256(r-1)r^3 + 27} \right) r^{14} + 7864320 \left(336\sqrt{3} - 55\sqrt{256(r-1)r^3 + 27} \right) r^{13} \\
& - 15925248 \left(16\sqrt{3} - 3\sqrt{256(r-1)r^3 + 27} \right) r^{12} - 10616832 \left(16\sqrt{3} - 3\sqrt{256(r-1)r^3 + 27} \right) r^{11} \\
& - 3981312 \left(109\sqrt{3} - 24\sqrt{256(r-1)r^3 + 27} \right) r^{10} + 5971968 \left(15\sqrt{3} - 4\sqrt{256(r-1)r^3 + 27} \right) r^9 \\
& + 3732480 \left(15\sqrt{3} - 4\sqrt{256(r-1)r^3 + 27} \right) r^8 + 2239488 \left(15\sqrt{3} - 4\sqrt{256(r-1)r^3 + 27} \right) r^7 \\
& - 2519424 \left(3\sqrt{3} - \sqrt{256(r-1)r^3 + 27} \right) r^6 - 1259712 \left(3\sqrt{3} - \sqrt{256(r-1)r^3 + 27} \right) r^5 \\
& \left. - 472392 \left(3\sqrt{3} - \sqrt{256(r-1)r^3 + 27} \right) r^4 \right]^{-1} \\
& \times \left\{ \left[-268435456 \left(12\sqrt{3} - \kappa_0 \right) r^{15} + 1006632960 \left(12\sqrt{3} - \kappa_0 \right) r^{14} - 1291845632 \left(12\sqrt{3} - \kappa_0 \right) r^{13} \right. \right. \\
& + 866123776 \left(12\sqrt{3} - \kappa_0 \right) r^{12} - 9437184 \left(1488\sqrt{3} - 139\kappa_0 \right) r^{11} + 1441792 \left(13524\sqrt{3} - 1397\kappa_0 \right) r^{10} \\
& - 786432 \left(12489\sqrt{3} - 1412\kappa_0 \right) r^9 + 2654208 \left(671\sqrt{3} - 118\kappa_0 \right) r^8 - 1327104 \left(3161\sqrt{3} - 584\kappa_0 \right) r^7 \\
& + 497664 \left(6763\sqrt{3} - 1282\kappa_0 \right) r^6 - 1492992 \left(78\sqrt{3} - 19\kappa_0 \right) r^5 + 186624 \left(831\sqrt{3} - 221\kappa_0 \right) r^4 \\
& \left. - 279936 \left(1527\sqrt{3} - 397\kappa_0 \right) r^3 + 6613488 \left(3\sqrt{3} - \kappa_0 \right) r^2 + 4408992 \left(3\sqrt{3} - \kappa_0 \right) r \right] \\
& + \left[28311552 \left(12\sqrt{3} - \kappa_0 \right) r^{14} - 42467328 \left(12\sqrt{3} - \kappa_0 \right) r^{13} + 5308416 \left(12\sqrt{3} - \kappa_0 \right) r^{12} \right. \\
& + 3538944 \left(12\sqrt{3} - \kappa_0 \right) r^{11} + 1327104 \left(129\sqrt{3} - 22\kappa_0 \right) r^{10} - 5971968 \left(9\sqrt{3} - 2\kappa_0 \right) r^9 \\
& - 3732480 \left(9\sqrt{3} - 2\kappa_0 \right) r^8 - 2239488 \left(9\sqrt{3} - 2\kappa_0 \right) r^7 + 2519424 \left(3\sqrt{3} - \kappa_0 \right) r^6 + 1259712 \left(3\sqrt{3} - \kappa_0 \right) r^5 \\
& \left. + 472392 \left(3\sqrt{3} - \kappa_0 \right) r^4 \right] \omega_{\alpha}^2 + 6613488 \left(3\sqrt{3} - \kappa_0 \right) \\
& + l^2 \left[268435456 \left(12\sqrt{3} - \kappa_0 \right) r^{16} - 939524096 \left(12\sqrt{3} - \kappa_0 \right) r^{15} + 1124073472 \left(12\sqrt{3} - \kappa_0 \right) r^{14} \right. \\
& - 469762048 \left(12\sqrt{3} - \kappa_0 \right) r^{13} + 4194304 \left(339\sqrt{3} - 62\kappa_0 \right) r^{12} - 2097152 \left(1599\sqrt{3} - 302\kappa_0 \right) r^{11} \\
& - 3932160 \left(591\sqrt{3} - 110\kappa_0 \right) r^{10} - 7077888 \left(9\sqrt{3} - 2\kappa_0 \right) r^9 + 884736 \left(153\sqrt{3} - 43\kappa_0 \right) r^8 \\
& - 1327104 \left(225\sqrt{3} - 59\kappa_0 \right) r^7 + 4478976 \left(3\sqrt{3} - \kappa_0 \right) r^6 + 2985984 \left(3\sqrt{3} - \kappa_0 \right) r^5 + 4478976 \left(3\sqrt{3} - \kappa_0 \right) r^4 \left. \right] \\
& + l \left[268435456 \left(12\sqrt{3} - \kappa_0 \right) r^{16} - 939524096 \left(12\sqrt{3} - \kappa_0 \right) r^{15} + 1124073472 \left(12\sqrt{3} - \kappa_0 \right) r^{14} \right. \\
& - 469762048 \left(12\sqrt{3} - \kappa_0 \right) r^{13} + 4194304 \left(339\sqrt{3} - 62\kappa_0 \right) r^{12} - 2097152 \left(1599\sqrt{3} - 302\kappa_0 \right) r^{11} \\
& + 3932160 \left(591\sqrt{3} - 110\kappa_0 \right) r^{10} - 7077888 \left(9\sqrt{3} - 2\kappa_0 \right) r^9 + 884736 \left(153\sqrt{3} - 43\kappa_0 \right) r^8 \\
& - 1327104 \left(225\sqrt{3} - 59\kappa_0 \right) r^7 + 4478976 \left(3\sqrt{3} - \kappa_0 \right) r^6 + 2985984 \left(3\sqrt{3} - \kappa_0 \right) r^5 + 4478976 \left(3\sqrt{3} - \kappa_0 \right) r^4 \left. \right] \\
& + \left[-1610612736i\sqrt{3}r^{17} + 5234491392i\sqrt{3}r^{16} - 5737807872i\sqrt{3}r^{15} + 2139095040i\sqrt{3}r^{14} \right. \\
& - 12582912i \left(149\sqrt{3} - 18\kappa_0 \right) r^{13} + 9437184i \left(445\sqrt{3} - 54\kappa_0 \right) r^{12} - 7077888i \left(347\sqrt{3} - 42\kappa_0 \right) r^{11} \\
& + 1769472i \left(15\sqrt{3} - 2\kappa_0 \right) r^{10} - 5308416i \left(111\sqrt{3} - 22\kappa_0 \right) r^9 + 3981312i \left(195\sqrt{3} - 38\kappa_0 \right) r^8 \\
& - 2985984i \left(9\sqrt{3} - 2\kappa_0 \right) r^7 - 2239488i \left(9\sqrt{3} - 2\kappa_0 \right) r^6 - 3359232i \left(27\sqrt{3} - 7\kappa_0 \right) r^5 \\
& \left. + 2519424i \left(3\sqrt{3} - \kappa_0 \right) r^4 + 1889568i \left(3\sqrt{3} - \kappa_0 \right) r^3 + 1417176i \left(3\sqrt{3} - \kappa_0 \right) r^2 \right] \omega_{\alpha} \Big\}. \tag{A. 6}
\end{aligned}$$

The coefficients α_n appearing in Eq.(5.10) are given by

$$\begin{aligned}
\alpha_1 &= \frac{i(r-1)^2}{r^2}, \\
\alpha_2 &= -\frac{(r-1)^2}{r^2}, \\
\alpha_3 &= -\frac{6(r-1)\sqrt{768r^4 - 768r^3 + 81}\omega_{\text{ae}}}{256r^5 - 256r^4 + 27r} \\
&\quad + \frac{16i(r-1)^2(16r^2 + 12r + 9)}{r^3(4r-3)(16r^2 + 8r + 3)\sqrt{256(r-1)r^3 + 27}\left[\sqrt{256(r-1)r^3 + 27} - 3\sqrt{3}\right]^3} \\
&\quad \times \left[16384r^8 - 32768r^7 + 16384r^6 + 8640r^4 + 576\sqrt{768(r-1)r^3 + 81}r^3 - 8640r^3 \right. \\
&\quad \left. - 81\sqrt{768(r-1)r^3 + 81} - 576\sqrt{768(r-1)r^3 + 81}r^4 + 729 \right], \\
\alpha_4 &= -\frac{27\omega_{\text{ae}}^2}{256r^4 - 256r^3 + 27} \\
&\quad - \frac{12i(128r^4 - 128r^3 + 27)\omega_{\text{ae}}}{r^2(4r-3)(16r^2 + 8r + 3)\sqrt{256(r-1)r^3 + 27}\left(\sqrt{256(r-1)r^3 + 27} - 3\sqrt{3}\right)^3} \\
&\quad \times \left[-1728r^4 - 64\sqrt{3}\kappa_0r^3 + 1728r^3 + 27\sqrt{3}\kappa_0 + 64\sqrt{3}\kappa_0r^4 - 243 \right] \\
&\quad + \frac{16(r-1)^2(1024(l^2 + l - 2)r^5 + 128(3l^2 + 3l - 4)r^4 + 2048l(l+1)r^6 + 384r^3 + 3024r^2 + 1512r + 567)}{(3-4r)^2r^4(16r^2 + 8r + 3)^2\sqrt{256(r-1)r^3 + 27}\left(\sqrt{256(r-1)r^3 + 27} - 3\sqrt{3}\right)^4} \\
&\quad \times \left(98304\sqrt{3}r^8 - 196608\sqrt{3}r^7 + 98304\sqrt{3}r^6 + 31104\sqrt{3}r^4 - 31104\sqrt{3}r^3 + 6912\kappa_0r^3 - 729\kappa_0 - 8192\kappa_0r^8 \right. \\
&\quad \left. + 16384\kappa_0r^7 - 8192\kappa_0r^6 - 6912\kappa_0r^4 + 2187\sqrt{3} \right). \tag{A. 7}
\end{aligned}$$

[1] B.P. Abbott, *et al.*, [LIGO/Virgo Scientific Collaborations], Observation of Gravitational Waves from a Binary Black Hole Merger, *Phys. Rev. Lett.* **116**, 061102 (2016).

[2] B.P. Abbott, *et al.*, [LIGO/Virgo Collaborations], GWTC-1: A Gravitational-Wave Transient Catalog of Compact Binary Mergers Observed by LIGO and Virgo during the First and Second Observing Runs, *Phys. Rev. X* **9**, 031040 (2019).

[3] B.P. Abbott, *et al.*, [LIGO/Virgo Collaborations], Open data from the first and second observing runs of Advanced LIGO and Advanced Virgo, *SoftwareX*, Volume 13, 100658 (2021).

[4] B.P. Abbott, *et al.*, [LIGO/Virgo Collaborations], GW190425: Observation of a Compact Binary Coalescence with Total Mass $\sim 3.4M_{\odot}$, *ApJL* **892** L3 (2020).

[5] B.P. Abbott, *et al.*, [LIGO/Virgo/KAGRA Collaborations], GWTC-3: Compact Binary Coalescences Observed by LIGO and Virgo During the Second Part of the Third Observing Run, arXiv:2111.03606v1 [gr-qc].

[6] C. J. Moore, R. H. Cole and C. P. L. Berry, Gravitational-wave sensitivity curves, *Class. Quantum. Grav.* **32**, 015014 (2015).

[7] Y. Gong, J. Luo and B. Wang, “Concepts and status of Chinese space gravitational wave detection projects,” *Nature Astron.* **5**, no.9, 881-889 (2021).

[8] E. Berti, V. Cardoso and A. O. Starinets, Quasinormal modes of black holes and black branes, *Class. Quantum. Grav.* **26**, 163001 (2009).

[9] E. Berti, K. Yagi, H. Yang, N. Yunes, Extreme gravity tests with gravitational waves from compact binary coalescences: (II) ringdown, *Gen. Relativ. Grav.* **50**, 49 (2018).

[10] E. Berti, K. Yagi, H. Yang, N. Yunes, Extreme gravity tests with gravitational waves from compact binary coalescences: (I) inspiral-merger, *Gen. Relativ. Grav.* **50**, 46 (2018).

[11] CE, <https://cosmicexplorer.org/>.

[12] ET Steering Committee Editorial Team, ET design report update 2020, ET-0007A- 20 (2020); <https://www.et-gw.eu/>.

[13] <https://www.lisamission.org>

[14] S. Liu, Y. Hu, *et al.*, Science with the TianQin observatory: Preliminary results on stellar-mass binary black holes, *Phys. Rev. D* **101**, 103027 (2020); C.-F. Shi, *et al.*, Science with the TianQin observatory: Preliminary results on testing the no-hair theorem with ringdown signals, *Phys. Rev. D* **100**, 044036 (2019).

[15] W.-H. Ruan, Z.-K. Guo, R.-G. Cai, Y.-Z. Zhang, Taiji Program: Gravitational-Wave Sources, *Int. J. Mod. Phys. A* **35**, No. 17, 2050075 (2020).

[16] S. Kawamura, *et al.*, Current status of space gravitational wave antenna DECIGO and B-DECIGO, [arXiv:2006.13545](https://arxiv.org/abs/2006.13545).

[17] S. Chandrasekhar, the mathematical theory of black holes, Oxford classic texts in the physical sciences (Oxford Press, Oxford, 1992).

[18] S. Iyer, Black-hole normal modes: A WKB approach. II. Schwarzschild black holes, *Phys. Rev. D* **35**, 12 (1987).

[19] S. Chandrasekhar, F. R. S., and S. Detweiler, The quasinormal modes of the Schwarzschild black hole, *Proc. R. Soc. Lond. A.* **344**, 411-452 (1975).

[20] S. Detweiler, BLACK HOLES AND GRAVITATIONAL WAVES. III. THE RESONANT FREQUENCIES OF ROTATING HOLES, *Astrophys. J.* **239**, 292-295 (1980).

[21] E. Seidel and S. Iyer, Black-hole normal modes: A WKB approach. IV. Kerr black holes, *Phys. Rev. D* **41**, 2 (1990).

[22] B. F. Schutz and C. M. Will, BLACK HOLE NORMAL MODES: A SEMIANALYTIC APPROACH, *Astrophys. J.* **291**, L33-L36 (1985).

[23] S. Iyer and C. M. Will, Black-hole normal modes: A WKB approach. I. Foundations and application of a higher-order WKB analysis of potential-barrier scattering, *Phys. Rev. D* **35**, 12 (1987).

[24] R. A. Konoplya, Quasinormal behavior of the D-dimensional Schwarzschild black hole and the higher order WKB approach, *Phys. Rev. D* **68**, 024018 (2003).

[25] J. Matyjasek and M. Opala, Quasinormal modes of black holes: The improved semianalytic approach, *Phys. Rev. D* **96**, 024011 (2017).

[26] X. Li and S.-P. Zhao, Quasinormal modes of a scalar and an electromagnetic field in Finslerian-Schwarzschild spacetime, *Phys. Rev. D* **101**, 124012 (2020).

[27] E. W. Leaver, An analytic representation for the quasinormal modes of Kerr black holes, *Proc. R. Soc. Lond. A.* **402**, 285-298 (1985).

[28] K. Lin and W.-L. Qian, A matrix method for quasinormal modes: Schwarzschild black holes in asymptotically flat and (anti-) de Sitter spacetimes, *Class. Quantum Grav.* **34**, 095004 (2017).

[29] R. A. Konoplya and A. Zhidenko, Quasinormal modes of black holes: From astrophysics to string theory, *Rev. Mod. Phys.* **83**, 793 (2011).

[30] C. Gundlach, R. H. Price and J. Pullin, Late-time behavior of stellar collapse and explosions. I. Linearized perturbations, *Phys. Rev. D* **49**, 883 (1994).

[31] B. Wang, C.-Y. Lin and C. Molina, Quasinormal behavior of massless scalar field perturbation in Reissner-Nordström anti-de Sitter spacetimes, *Phys. Rev. D* **70**, 064025 (2004).

[32] X. Li and S.-P. Zhao, Quasinormal modes of a scalar and an electromagnetic field in Finslerian-Schwarzschild spacetime, *Phys. Rev. D* **101**, 124012 (2020).

[33] O. J. Tattersall and P. G. Ferreira, Forecasts for low spin black hole spectroscopy in Horndeski gravity, *Phys. Rev. D* **99**, 104082 (2019).

[34] H. Yang, D. A. Nichols, F. Zhang, *et al.*, Quasinormal-mode spectrum of Kerr black holes and its geometric interpretation, *Phys. Rev. D* **86**, 104006 (2012).

[35] T. Jacobson and D. Mattingly, Gravity with a dynamical preferred frame, *Phys. Rev. D* **64**, 024028 (2001).

[36] T. Jacobson, Einstein-æther gravity: a status report, *Proc. Sci., QG-PH* (2007) 020 [[arXiv:0801.1547v2](https://arxiv.org/abs/0801.1547v2)].

[37] J. Oost, S. Mukohyama and A. Wang, Constraints on æ-theory after GW170817, *Phys. Rev. D* **97**, 124023 (2018).

[38] O. Sarbach, E. Barausse, and J.A Preciado-López, Well-posed Cauchy formulation for Einstein-æther theory, *Class. Quantum Grav.* **36** (2019) 165007.

[39] D. Garfinkle and T. Jacobson, A Positive-Energy Theorem for Einstein-Aether and Hořava Gravity, *Phys. Rev. Lett.* **107**, 191102 (2011).

[40] B. Z. Foster, Radiation Damping in Einstein-Aether Theory, [arXiv:gr-qc/0602004v5](https://arxiv.org/abs/gr-qc/0602004v5).

[41] B. Z. Foster, *Phys. Rev. D* **76**, 084033 (2007).

[42] K. Yagi, D. Blas, N. Yunes and E. Barausse, “Strong Binary Pulsar Constraints on Lorentz Violation in Gravity,” *Phys. Rev. Lett.* **112**, 161101 (2014).

[43] K. Yagi, D. Blas, E. Barausse, and N. Yunes, *Phys. Rev. D* **89**, 084067 (2014).

[44] D. Hansen, N. Yunes, and K. Yagi, *Phys. Rev. D* **91**, 082003 (2015).

[45] Y.-G. Gong, S.-Q. Hou, D.-C. Liang, E. Papantonopoulos, *Phys. Rev. D* **97**, 084040 (2018).

[46] K. Lin, X. Zhao, C. Zhang, K. Lin, T. Liu, B. Wang, S.-J. Zhang, X. Zhang, W. Zhao, T. Zhu, A. Wang, *Phys. Rev. D* **99**, 023010 (2019).

[47] X. Zhao, C. Zhang, K. Lin, T. Liu, R. Niu, B. Wang, S.-J. Zhang, X. Zhang, W. Zhao, T. Zhu, A. Wang, Gravitational waveforms and radiation powers of the triple system PSR J0337+1715 in modified theories of gravity, *Phys. Rev. D* **100**, 083012 (2019).

[48] C. Zhang, X. Zhao, A. Wang, B. Wang, K. Yagi, N. Yunes, W. Zhao and T. Zhu, Gravitational waves from the quasicircular inspiral of compact binaries in Einstein-aether theory, *Phys. Rev. D* **101**, 044002 (2020).

[49] J. Oost, S. Mukohyama, A. Wang, Spherically symmetric exact vacuum solutions in Einstein-aether theory, *Universe* **7** (2021) 272 [[arXiv:2106.09044](https://arxiv.org/abs/2106.09044)].

[50] T. Gupta, M. Herrero-Valea, D. Blas, E. Barausse, N. Cornish, K. Yagi, N. Yunes, New binary pulsar constraints on Einstein-æther theory after GW170817, *Class. Quantum Grav.* **38**, 195003 (2021).

[51] C. Eling and T. Jacobson, Spherical Solutions in Einstein-Aether Theory: Static Aether and Stars, *Class. Quantum. Grav.* **23**, 5625 (2006).

[52] C. Eling and T. Jacobson, Black holes in Einstein-aether theory, *Class. Quantum. Grav.* **23**, 5643 (2006).

[53] T. Tamaki and U. Miyamoto, Generic features of Einstein-Aether black holes, *Phys. Rev. D* **77**, 024026 (2008).

[54] D. Blas and S. Sibiryakov, Hořava gravity versus thermodynamics: The black hole case, *Phys. Rev. D* **84**,

124043 (2011).

[55] E. Barausse, T. Jacobson and T.P. Sotiriou, Black holes in Einstein-aether and Hořava-Lifshitz gravity, *Phys. Rev. D* **83**, 124043 (2011).

[56] P. Berglund, J. Bhattacharyya and D. Mattingly, Mechanics of universal horizons, *Phys. Rev. D* **85**, 124019 (2012).

[57] A. Wang, Stationary and slowly rotating spacetimes in Hořava-Lifshitz gravity, *Phys. Rev. Lett.* **110**, 091101 (2013).

[58] C. Ding, A. Wang and X. Wang, Charged Einstein-aether black holes and Smarr formula, *Phys. Rev. D* **92**, 084055 (2015).

[59] C. Zhang, X. Zhao, K. Lin, S.-J. Zhang, W. Zhao and A.-Z. Wang, Spherically symmetric static black holes in Einstein-aether theory, *Phys. Rev. D* **102**, 064043 (2020).

[60] A. Adam, P. Figueras, T. Jacobson, and T. Wiseman, Rotating black holes in Einstein-aether theory, arXiv:2108.00005.

[61] R. Chan, M. F. A. da Silva, V. H. Satheeshkumar, Thermodynamics of Einstein-Aether Black Holes, arXiv:2112.14978.

[62] M. Bhattacharjee, S. Mukohyama, M.-B. Wan, and A. Wang, Gravitational collapse and formation of universal horizons in Einstein-æther theory, *Phys. Rev. D* **98**, 064010 (2018).

[63] D. Garfinkle, C. Eling, and T. Jacobson, Numerical simulations of gravitational collapse in Einstein-aether theory, *Phys. Rev. D* **76**, 024003 (2007).

[64] T. Clifton, P.G. Ferreira, A. Padilla, C. Skordis, Modified Gravity and Cosmology, *Phys. Reports* **513**, 1 (2012).

[65] D. Langlois, Dark energy and modified gravity in degenerate higher-order scalar-tensor (DHOST) theories: A review, *Inter. J. Mod. Phys. D* **28**, 1942006 (2019).

[66] A. Bourgois, et al., Constraining velocity-dependent Lorentz and CPT violations using lunar laser ranging, *Phys. Rev. D* **103**, 064055 (2021).

[67] H. Pihan-le Bars, et al., New Test of Lorentz Invariance Using the MICROSCOPE Space Mission, *Phys. Rev. Lett.* **123**, 231102 (2019).

[68] C.G. Shao, et al., Combined Search for a Lorentz-Violating Force in Short-Range Gravity Varying as the Inverse Sixth Power of Distance, *Phys. Rev. Lett.* **122**, 011102 (2019).

[69] A. Bourgois, C. Le Poncin-Lafitte, A. Hees, S. Bouquillon, G. Francou, and M.-C. Angonin, Lorentz Symmetry Violations from Matter-Gravity Couplings with Lunar Laser Ranging, *Phys. Rev. Lett.* **119**, 201102 (2017).

[70] N.A. Flowers, C. Goodge, and J.D. Tasson, Superconducting-Gravimeter Tests of Local Lorentz Invariance, *Phys. Rev. Lett.* **119**, 201101 (2017).

[71] A. Kostelecký and N. Russell, Data tables for Lorentz and CPT violation, *Rev. Mod. Phys.* **83** 11 (2011) [arXiv:0801.0287v15, January 2022 Edition].

[72] J. Collins, A. Perez, D. Sudarsky, L. Urrutia, and H. Vucetich, Lorentz invariance and quantum gravity: an additional fine-tuning problem?, *Phys. Rev. Lett.* **93** (2004) 191301.

[73] D. Mattingly, Modern Tests of Lorentz Invariance, *Living Rev. Relativity*, **8**, 5 (2005).

[74] S. Liberati, Tests of Lorentz invariance: a 2013 update, *Class. Quantum Grav.* **30**, 133001 (2013).

[75] M. Pospelov and C. Tamarit, Lifshitz-sector mediated SUSY breaking, *J. High Energy Phys.* **01** (2014) 048.

[76] A. Wang, Hořava gravity at a Lifshitz point: A progress report, *Inter. J. Mod. Phys. D* **26**, 1730014 (2017).

[77] T. Jacobson and D. Mattingly, Einstein-aether waves, *Phys. Rev. D* **70**, 024003 (2004).

[78] J. W. Elliott, G. D. Moore and H. Stoica, Constraining the New Aether: Gravitational Cherenkov Radiation, *JHEP* **0508**, 066 (2005).

[79] J. Calderón Bustillo, P.D. Lasky, and E. Thrane, Black-hole spectroscopy, the no-hair theorem, and GW150914: Kerr versus Occam, *Phys. Rev. D* **103**, 024041 (2021).

[80] R. Abbott, et al. [The LIGO and Virgo Collaborations], Tests of general relativity with binary black holes from the second LIGO-Virgo gravitational-wave transient catalog, *Phys. Rev. D* **103**, 122002 (2021).

[81] X. J. Forteza, S. Bhagwat, P. Pani, and V. Ferrari, Spectroscopy of binary black hole ringdown using overtones and angular modes, *Phys. Rev. D* **102**, 044053 (2020).

[82] S. Bhagwat, X. J. Forteza, P. Pani, and V. Ferrari, Ringdown overtones, black hole spectroscopy, and no-hair theorem tests, *Phys. Rev. D* **101**, 044033 (2020).

[83] M. Giesler, M. Isi, M. Scheel, and S. Teukolsky, Black Hole Ringdown: The Importance of Overtones, *Phys. Rev. X* **9**, 041060 (2019).

[84] M. Isi, M. Giesler, W. M. Farr, M. A. Scheel, and S. A. Teukolsky, Testing the No-Hair Theorem with GW150914, *Phys. Rev. Lett.* **123**, 111102 (2019).

[85] G. Carullo, W. Del Pozzo, and J. Veitch, Observational black hole spectroscopy: A time-domain multi-mode analysis of GW150914, *Phys. Rev. D* **99**, 123029 (2019).

[86] C.D. Capano and A.H. Nitz, Binary black hole spectroscopy: A no-hair test of GW190814 and GW190412, *Phys. Rev. D* **102**, 124070 (2020).

[87] I. Ota and C. Chirenti, Overtones or higher harmonics? Prospects for testing the no-hair theorem with gravitational wave detections, *Phys. Rev. D* **101**, 104005 (2020).

[88] F.H. Shaik, J. Lange, S.E. Field, R. O'Shaughnessy, V. Varma, L.E. Kidder, H.P. Pfeiffer, and D. Wysocki, Impact of subdominant modes on the interpretation of gravitational-wave signals from heavy binary black hole systems, *Phys. Rev. D* **101**, 124054 (2020).

[89] N. Uchikata, T. Narikawa, K. Sakai, H. Takahashi, and Hiroyuki Nakano, Black hole spectroscopy for KAGRA future prospect in O5, *Phys. Rev. D* **102**, 024007 (2020).

[90] S. Bhagwat, M. Cabero, C.D. Capano, B. Krishnan, and D.A. Brown, Detectability of the subdominant mode in a binary black hole ringdown, *Phys. Rev. D* **102**, 024023 (2020).

[91] M. Cabero, J. Westerweck, C.D. Capano, S. Kumar, A.B. Nielsen, and B. Krishnan, Black hole spectroscopy in the next decade, *Phys. Rev. D* **101**, 064044 (2020).

[92] A. Maselli, P. Pani, L. Gualtieri, and E. Berti, Parametrized ringdown spin expansion coefficients: A data-analysis framework for black-hole spectroscopy with multiple events, *Phys. Rev. D* **101**, 024043 (2020).

[93] T. Islam, A.K. Mehta, A. Ghosh, V. Varma, P. Ajith, and B.S. Sathyaprakash, Testing the no-hair nature of binary black holes using the consistency of multipolar gravitational radiation, *Phys. Rev. D* **101**, 024032 (2020).

[94] B. P. Abbott, et al., [LIGO/Virgo/KAGRA Collaborations], Tests of General Relativity with GWTC-3,

arXiv:2112.06861v1 [gr-qc].

[95] S. Tsujikawa, C. Zhang, X. Zhao, A. Wang, Odd-parity stability of black holes in Einstein-Aether gravity, *Phys. Rev. D* **104**, 064024 (2021).

[96] B. P. Abbott et al. [LIGO Scientific and Virgo Collaborations], GW170817: Observation of Gravitational Waves from a Binary Neutron Star Inspiral, *Phys. Rev. Lett.* **119**, 161101 (2017).

[97] A. Goldstein et al., An Ordinary Short Gamma-Ray Burst with Extraordinary Implications: Fermi-GBM Detection of GRB 170817A, *Astrophys. J.* **848**, L14 (2017).

[98] S. M. Carroll and E. A. Lim, Lorentz-violating vector fields slow the universe down, *Phys. Rev. D* **70**, 123525 (2004).

[99] J. Müller, J.G. Williams and S.G. Turyshev, Lunar laser ranging contributions to relativity and geodesy, *Astrophys. Space Sci. Libr.* **349** (2008) 457.

[100] J. Greenwald, J. Lenells, J.-X. Lu, V.H. Satheeshkumar, A. Wang, Black holes and global structures of spherical spacetimes in Hořava-Lifshitz theory, *Phys. Rev. D* **84**, 084040 (2011). 5

[101] D. Blas, O. Pujolas, and S. Sibiryakov, A healthy extension of Hořava gravity, *Phys. Rev. Lett.* **104**, 181302 (2010).

[102] D. Blas, O. Pujolas, and S. Sibiryakov, Models of non-relativistic quantum gravity: the good, the bad and the healthy, *JHEP* **04** (2011) 018.

[103] P. Hořava, Membranes at quantum criticality, *JHEP* **0903** (2009) 020; Quantum gravity at a Lifshitz point, *Phys. Rev. D* **79**, 084008 (2009).

[104] K. Lin, E. Abdalla, R.-G. Cai and A. Wang, Universal horizons and black holes in gravitational theories with broken Lorentz symmetry, *Int. J. Mod. Phys. D* **23**, 1443004 (2014).

[105] T. Jacobson, Undoing the twist: The Horava limit of Einstein-aether theory, *Phys. Rev. D* **89**, 081501(R) (2014); *Phys. Rev. D* **81**, 101502 (2010); Extended Horava gravity and Einstein-aether theory, *Phys. Rev. D* **81**, 101502(R) (2010); *D* **82**, 129901(E) (2010).

[106] R. M. Wald, *General Relativity* (University of Chicago Press, 2010).

[107] K. Lin, V.H. Satheeshkumar, and A. Wang, Static and rotating universal horizons and black holes in gravitational theories with broken Lorentz invariance, *Phys. Rev. D* **93**, 124025 (2016).

[108] K. Lin, O. Goldoni, M.F. da Silva, and A. Wang, A New Look at Those Old Black Holes: Existence of Universal Horizons, *Phys. Rev. D* **91**, 024047 (2015).

[109] J. E. Thompson, H. Chen and B. F. Whiting, Gauge invariant perturbations of the Schwarzschild spacetime, *Class. Quantum Grav.* **34** 174001 (2017).

[110] T. Regge and J. A. Wheeler, Stability of a Schwarzschild Singularity, *Phys. Rev.* **108**, 4 (1957).

[111] R. d' Inverno, *Introducing Einstein's Relativity* (Oxford University Press, New York, 2000).

[112] E. Butkov, *Mathematical Physics* (Addison-Wesley Publishing Company, Canada, 1972).

[113] C. Zhang, T. Zhu and A. Wang, Gravitational axial perturbations of Schwarzschild-like black holes in dark matter halos, *Phys. Rev. D* **104**, 124082 (2021); C. Zhang, T. Zhu, X. Fang and A. Wang, Imprints of dark matter on gravitational ringing of supermassive black holes, *Phys. Dark Univ.* **37**, 10107 (2022).

[114] A. Ghosh, R. Brito and A. Buonanno, Constraints on quasinormal-mode frequencies with LIGO-Virgo binary-black-hole observations, *Phys. Rev. D* **103**, 124041 (2021).